Article

Base-Pairing, Tautomerism, and Mismatch Discrimination of 7-Halogenated 7-Deaza-2'-deoxyisoguanosine: Oligonucleotide Duplexes with Parallel and Antiparallel Chain Orientation

Frank Seela, Xiaohua Peng, and Hong Li

J. Am. Chem. Soc., **2005**, 127 (21), 7739-7751• DOI: 10.1021/ja0425785 • Publication Date (Web): 06 May 2005

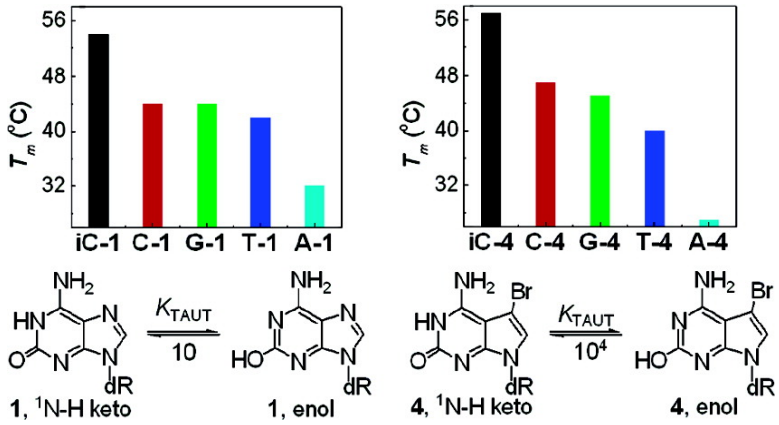

More About This Article

Additional resources and features associated with this article are available within the HTML version:

- Supporting Information
- Links to the 4 articles that cite this article, as of the time of this article download
- Access to high resolution figures
- Links to articles and content related to this article
- Copyright permission to reproduce figures and/or text from this article

View the Full Text HTML

J|A|C|S
ARTICLES
Published on Web 05/06/2005

Base-Pairing, Tautomerism, and Mismatch Discrimination of 7-Halogenated 7-Deaza-2′-deoxyisoguanosine: Oligonucleotide Duplexes with Parallel and Antiparallel Chain Orientation

Frank Seela,* Xiaohua Peng, and Hong Li

Contribution from the Laboratorium für Organische und Bioorganische Chemie, Institut für Chemie, Universität Osnabrück, Barbarastrasse 7, D-49069 Osnabrück, Germany, and Laboratory of Bioorganic and Biophysical Chemistry, Center for Nanotechnology, Gievenbecker Weg 11, 48149 Münster, Germany

Received December 10, 2004; E-mail: Frank.Seela@uni-osnabrueck.de

Abstract: Oligonucleotides containing 2′-deoxyisoguanosine (**1**, iG_d), 7-deaza-2′-deoxyisoguanosine (**2**, c^7iG_d), and its 7-halogenated derivatives **3** and **4** were synthesized on solid phase using the phosphoramidite building blocks **5**−**7**. The hybridization properties of oligonucleotides were studied on duplexes with parallel and antiparallel chain orientation. It was found that the 7-halogenated nucleoside analogues **3** and **4** enhance the duplex stability significantly in both parallel (ps) and antiparallel (aps) DNA. Moreover, the halogenated nucleosides shift the tautomeric keto−enol equilibrium strongly toward the keto form, with K_{TAUT} [keto]/[enol] $\approx 10^4$ coming close to that of 2′-deoxyguanosine (10^4−10^5), while the nonhalogenated 7-deaza-2′-deoxyisoguanosine **2** shows a K_{TAUT} of around 2000 and the enol concentration of **1** is 10% in aqueous solution. Consequently, nucleosides **3** and **4** show a much better mismatch discrimination against dT than compound **1** or **2** in antiparallel as well as in parallel DNA. **3** and **4** are expected to increase the selectivity of base incorporation opposite to $isoC_d$ in the form of triphosphates or in the polymerase-catalyzed reaction in comparison to **1** or **2**.

Introduction

The polymorphic nature of double-stranded DNA is well-established.[1] The antiparallel strand orientation is the common feature of the three major families of A-, B-, and Z-DNA. A recent addition to the well-known DNA families is that of parallel-stranded (ps) DNAs.[2] This type of duplex formation may offer new opportunities for designing new oligonucleotide hybridization probes, antisense constructs, or interference RNA mimics.[3] ps-DNA can be constructed from oligonucleotides containing reverse Watson−Crick adenine−thymine base pair[2] and isoguanine−cytosine or guanine−isocytosine pairs instead of the canonical guanine−cytosine pair.[4] The thermodynamic stability of ps-DNA when formed exclusively by dA−dT base pairs is lower than that of the corresponding aps-DNA,[2] while 2′-deoxyisoguanosine (**1**, iG_d)[4f,g] can stabilize ps-DNA by forming three hydrogen bonds with 2′-deoxycytidine (dC).[4b,c] Therefore, 2′-deoxyisoguanosine has attracted much attention as inducer of ps-DNA. On the other hand, in aps-DNA, iG_d forms a stable Watson−Crick base pair with 2′-deoxyisocytidine (iC_d), which can be incorporated into duplex DNA by polymerases, thereby expanding the genetic alphabet from four to six letters.[5,6] However, it has been shown that the incorporation of 2′-deoxyisoguanosine triphosphates opposite to iC_d in DNA causes the formation of iG_d−dT mismatches during replication.[5a,7,8] This has been correlated to a particular property of

(1) (a) *DNA Topology and Its Biological Effects*; Cozzarelli, N. R., Wang, J. C., Eds.; Cold Spring Harbor Laboratory Press: New York, 1990. (b) *DNA Structure and Function*; Sinden, R. R., Ed.; Academic Press: New York, 1994.
(2) van de Sande, J. H.; Ramsing, N. B.; Germann, M. W.; Elhorst, W.; Kalisch, B. W.; von Kitzing, E.; Pon, R. T.; Clegg, R. C.; Jovin, T. M. *Science* **1988**, *241*, 551−557.
(3) (a) Rippe, K.; Fritsch, V.; Westhof, E.; Jovin, T. M. *EMBO J.* **1992**, *11*, 3777−3786. (b) Marfurt, J.; Leumann, C. *Angew. Chem., Int. Ed.* **1998**, *37*, 175−177.
(4) (a) Seela, F.; Gabler, B.; Kazimierczuk, Z. *Collect. Czech. Chem. Commun.* **1993**, *58*, 170−173. (b) Sugiyama, H.; Ikeda, S.; Saito, I. *J. Am. Chem. Soc.* **1996**, *118*, 9994−9995. (c) Seela, F.; Wei, C. *Helv. Chim. Acta* **1997**, *80*, 73−85. (d) Seela, F.; He, Y.; Wei, C. *Tetrahedron* **1999**, *55*, 9481−9500. (e) Yang, X.-L.; Sugiyama, H.; Ikeda, S.; Saito, I.; Wang, A. H.-J. *Biophys. J.* **1998**, *75*, 1163−1171. (f) Kazimierczuk, Z.; Mertens, R.; Kawczynski, W.; Seela, F. *Helv. Chim. Acta* **1991**, *74*, 1742−1748. (g) Seela, F.; Gabler, B. *Helv. Chim. Acta* **1994**, *77*, 622−630. (h) Seela, F.; Fröhlich, T. *Collect. Czech. Chem. Commun.* **1993**, *58*, 183−186. (i) Seela, F.; Wei, C. *Collect. Czech. Chem. Commun.* **1996**, *61*, 114−115. (j) Li, H.; Peng, X.; Seela, F. *Bioorg. Med. Chem. Lett.* **2004**, *14*, 6031−6034.
(5) (a) Switzer, C.; Moroney, S. E.; Benner, S. A. *J. Am. Chem. Soc.* **1989**, *111*, 8322−8323. (b) Piccirilli, J. A.; Krauch, T.; Moroney, S. E.; Benner, S. A. *Nature* **1990**, *343*, 33−37. (c) Bain, J. D.; Switzer, C.; Chamberlin, A. R.; Benner, S. A. *Nature* **1992**, *356*, 537−539. (d) Roberts, C.; Bandaru, R.; Switzer, C. *J. Am. Chem. Soc.* **1997**, *119*, 4640−4649. (e) Rice, K. P.; Chaput, J. C.; Cox, M. M.; Switzer, C. *Biochemistry* **2000**, *39*, 10177−10188. (f) Tor, Y.; Dervan, P. B. *J. Am. Chem. Soc.* **1993**, *115*, 4461−4467.
(6) Johnson, S. C.; Sherrill, C. B.; Marshall, D. J.; Moser, M. J.; Prudent, J. R. *Nucleic Acids Res.* **2004**, *32*, 1937−1941.
(7) Switzer, C. Y.; Moroney, S. E.; Benner, S. A. *Biochemistry* **1993**, *32*, 10489−10496.
(8) (a) Kamiya, H.; Kasai, H. *FEBS Lett.* **1996**, *391*, 113−116. (b) Kamiya, H.; Ueda, T.; Ohgi, T.; Matsukage, A.; Kasai, H. *Nucleic Acids Res.* **1995**, *23*, 761−766.

the isoguanine base that adopts the form of an enol tautomer much more easily than the canonical DNA nucleobases.[9,10] Earlier, Shugar and co-worker examined the properties of iG_d by optical methods and concluded that although iG_d favors the keto (N1−H) form in aqueous solution, the enol tautomer is present to a significant amount (10%).[10] Crystallographic data of a Watson−Crick iG_d−dT pair with isoguanine in the enol form observed by Wang and co-workers provide the most direct evidence to date in support of iG_d infidelity resulting from the enol−keto tautomerism.[11] This situation makes the fidelity of replication and translation inherently more difficult to control for any genetic system bearing iG_d. Thus, the ambiguity of base pairing caused by tautomerism limits the use of iG_d as a "letter in the genetic alphabet" and can cause mutagenic events during replication.

To find an ideal candidate as a new member of "letters of the genetic alphabet", two special targets for a modified nucleoside should be met: (i) a high thermodynamic stability of the iG_d−dC (or iG_d−iC_d) base pair and (ii) a neglectible content of the iG_d enol form decreasing the probability of mutagenesis during replication. Since the keto−enol equilibrium of iG_d depends on the polarity of its microenvironment, one can expect that the modification of nucleobases would influence this equilibrium, resulting in an alteration of the coding properties. Earlier, we reported on the replacement of the imidazole moiety of **1** by a pyrrole ring leading to 7-deaza-2′-deoxyisoguanosine (**2**)[12] (purine numbering is used throughout the discussion and systematic numbering is used in the experiment part). Recently, Benner and co-workers observed that the keto form in compound **2** is more favored (K_{TAUT} = [keto]/[enol] ≈ 10^3, room temperature, aqueous solution) than that in 2′-deoxyisoguanosine (K_{TAUT} ≈ 10).[13] Nevertheless, experimental data obtained from DNA melting curves indicate that the thermodynamic stability of duplexes containing **2**−dC pairs are indeed somewhat lower than that containing an iG_d−dC pair,[12a,14a] which in turn is less stable than the dG−dC pair in aps-DNA. Moreover, compound **2** shows base-pair ambiguity as it is observed for **1**.[12a,14b]

It has already been shown that the introduction of 7-substituents into 7-deazapurines results in a stabilization of oligonucleotide duplexes with antiparallel or parallel chain orientation.[15,16] Also, chemical modification of the base, in particular the addition of an electronegative atom to the heterocycles, can produce bases with significantly altered tautomeric ratios.[17] Recently, we reported on the synthesis

Scheme 1. Structure of Nucleosides and Phosphoramidite Building Blocks

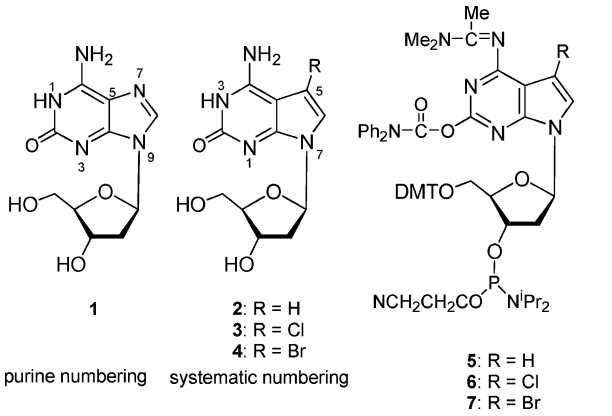

of 7-halogenated 7-deaza-2′-deoxyisoguanosine analogues **3** ($Cl^7c^7iG_d$) and **4** ($Br^7c^7iG_d$) bearing halogen substituents at C-7 with the potential to enhance duplex stability.[18] The introduction of halogen substituents might also affect the tautomerism of **3** and **4**. Herein, nucleosides **2**−**4** have been converted into the phosphoramidites building blocks **5**−**7**, which were employed in solid-phase oligonucleotide synthesis (Scheme 1). The tautomerism of nucleosides **3** and **4** was studied, and base-pairing properties (stability and selectivity) were investigated in DNA with parallel and antiparallel chain orientation.

Results and Discussion

Monomers. The 7-deazaisoguanine nucleosides **2**−**4** were prepared from the corresponding 7-deazapurin-2,6-diamine nucleosides **8**−**10** (Scheme 2).[12a,18] The next task was to choose protecting groups for the nucleobase amino and oxo functions that could survive in automated oligonucleotide synthesis and remain labile to postsynthetic treatment with concentrated aqueous ammonia. As the isobutyryl (^{i}Bu) residue had already been successfully employed in the case of compound **2**,[12a] the initial choice for the 6-amino protection of nucleosides **3** and **4** was the isobutyryl residue. Unfortunately, during the stage of removing the transient silyl OH-protecting group by aqueous ammonia the ^{i}Bu residue was also lost. Only 10% of the desired product **12** was obtained, and 77% of starting material **11** was recovered (Scheme 2). Apparently, the 7-bromo substituent of **4** increases the acidic character of the 6-amino group, thereby destabilizing the protecting group. This is underlined by the half-life for deprotection of **12** (τ = 4 min) compared to 60 min in the case of compound **2**[12a] (Table 1 and Supporting Information).

Earlier, the *N*,*N*-dimethylaminoethylidene residue was chosen for protecting the 6-amino group of 2′-deoxyisoguanosine.[4c] Thus, the amino groups of compounds **2**−**4** were protected with the *N*,*N*-dimethylaminoethylidene residue using dimethylacetamide dimethylacetal/MeOH to yield the amino-protected compounds **13a**−**c** in 89−91% yield (Scheme 3). It has been shown that in the case of isoguanosine derivatives, the 2-oxo-unprotected phosphoramidite resulted in inefficient coupling yields. The protection of the 2-oxo group with a diphenylcarbamoyl residue resulted in significantly higher coupling yields during oligonucleotide synthesis.[12a] Likewise, the nucleosides **13a**−**c** were treated with diphenylcarbamoyl chloride (dpc-Cl) in pyridine to furnish the 2-oxo-protected nucleosides **14a**−**c**.

(9) Seela, F.; Wei, C.; Kazimierczuk, Z. *Helv. Chim. Acta* **1995**, *78*, 1843−1854.
(10) Sepiol, J.; Kazimierczuk, Z.; Shugar, D. *Z. Naturforsch. C* **1976**, *31*, 361−370.
(11) Robinson, H.; Gao, Y.-G.; Bauer, C.; Roberts, C.; Switzer, C.; Wang, A. H.-J. *Biochemistry* **1998**, *37*, 10897−10905.
(12) (a) Seela, F.; Wei, C. *Helv. Chim. Acta* **1999**, *82*, 726−745. (b) Seela, F.; Wei, C.; Reuter, H.; Kastner, G. *Acta Crystallogr.* **1999**, *C55*, 1335−1337.
(13) Martinot, T. A.; Benner, S. A. *J. Org. Chem.* **2004**, *69*, 3972−3975.
(14) (a) Seela, F.; Wei, C.; Melenewski, A.; He, Y.; Kröschel, R.; Feiling, E. *Nucleosides Nucleotides* **1999**, *18*, 1543−1548. (b) Kawakami, J.; Kamiya, H.; Yasuda, K.; Fujiki, H.; Kasai, H.; Sugimoto, N. *Nucleic Acids Res.* **2001**, *29*, 3289−3296.
(15) (a) Seela, F.; Thomas, H. *Helv. Chim. Acta* **1995**, *78*, 94−108. (b) Seela, F.; Zulauf, M. *Chem.−Eur. J.* **1998**, *4*, 1781−1790.
(16) (a) Ramzaeva, N.; Seela, F. *Helv. Chim. Acta* **1996**, *79*, 1549−1558. (b) Aubert, Y.; Perrouault, L.; Hélène, C.; Giovannangeli, C.; Asseline, U. *Bioorg. Med. Chem.* **2001**, *9*, 1617−1624.
(17) (a) Kwiatkowski, J. S.; Pullman, B. In *Advances in Heterocyclic Chemistry*; Katritzky, A. R., Boulton, A. J., Eds.; Academic Press: New York, 1975; Volume 18, pp 199−335. (b) Hill, F.; Williams, D. M.; Loakes, D.; Brown, D. M. *Nucleic Acids Res.* **1998**, *26*, 1144−1149.
(18) Seela, F.; Peng, X. *Synthesis* **2004**, 1203−1210.

Scheme 2. Synthetic Route for the Preparation of Compounds **2**−**4**, **11**, and **12**[a]

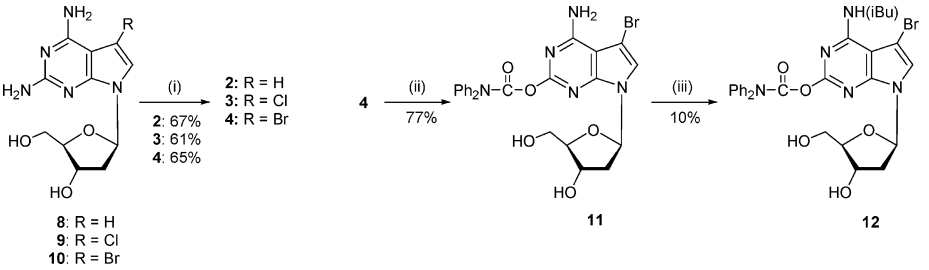

[a] (i) Sodium nitrite, AcOH/H_2O (v/v 1:5), room temperature, 30 min; (ii) diphenylcarbamoyl chloride, pyridine, *N*,*N*-diisopropylethylamine; (iii) Me_3SiCl, ^{i}BuCl, pyridine, room temperature, 3 h; aqueous NH_3, 0 °C.

Table 1. Half-Life Values (τ) for the Deprotection of 7-Deaza-2′-deoxyisoguanosine Derivatives in 25% Aqueous Ammonia at 40 °C

compd	UV λ (nm)	half-life τ (min)	compd	UV λ (nm)	half-life τ (min)
11	275	66	**13c**	315	310
12	303	4 (^{i}Bu), 74 (dpc)[a]	**14a**[b]	313	92
13a	313	260	**14b**[b]	315	109
13b	315	292	**14c**[b]	315	132

[a] Supporting Information. [b] Apparent half-lives.

Scheme 3. Synthesis of the 7-Deazaisoguanine Nucleoside Building Blocks for DNA Synthesis[a]

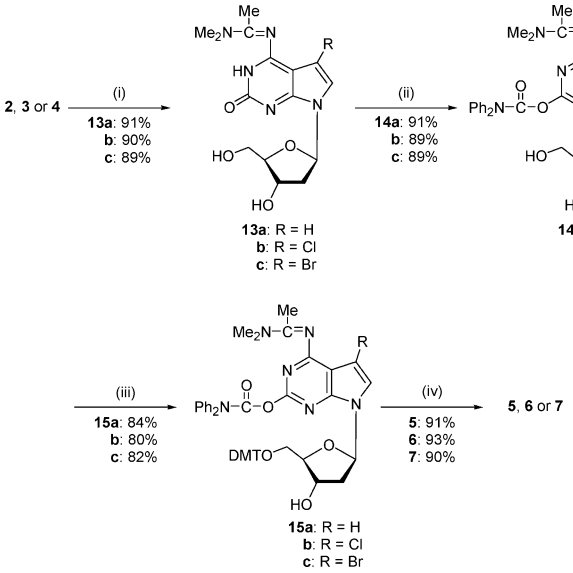

[a] (i) Dimethylacetamide dimethylacetal, MeOH, room temperature, 30 min; (ii) diphenylcarbamoyl chloride, anhydrous pyridine, *N*,*N*-diisopropylethylamine; (iii) 4,4′-dimethoxytriphenylmethyl chloride, anhydrous pyridine, room temperature; (iv) 2-cyanoethyl-*N*,*N*-diisopropylchlorophosphoramidite, *N*,*N*-diisopropylethylamine, CH_2Cl_2.

The stability of the protecting groups (**13a**−**c** and **14a**−**c**) was studied UV-spectrophotometrically in 25% aqueous NH_3 at 40 °C (Table 1). The acetamidine derivatives **13a**−**c** (τ: 260−310 min) are rather stable, whereas the ^{i}Bu-protected nucleoside **12** (τ: 4 min) is too labile. However, the combination of the protecting groups on compounds **14a**−**c** was found to be suitable for further manipulations, including oligonucleotide deprotection under basic conditions. Subsequently, compounds **14a**−**c** were converted into the 5′-*O*-DMT derivatives **15a**−**c** under standard conditions. Phosphitylation of the DMT derivatives **15a**−**c** was performed in anhydrous CH_2Cl_2 in the presence of ^{i}Pr_2EtN and 2-cyanoethyl-*N*,*N*-diisopropylchlorophosphoramidite, furnishing the phosphoramidites **5**−**7** (Scheme 3). In the case of the nonfunctionalized compound **2**, the route discussed above is superior to that described by Seela et al.,[12a] which used the ^{i}Bu residue for the 6-amino group protection, giving only a total yield of 36%.

The structures of all new compounds were confirmed by ^{1}H-, ^{13}C-, or ^{31}P NMR spectroscopy as well as by elemental analysis (see Experimental Section). The ^{13}C NMR chemical shift assignment was made according to gated-decoupled ^{13}C NMR spectra (Table 2). Compared to the nonhalogenated compounds **2**, **13a**, **14a**, and **15a**, the 7-bromo substituent (compounds **4**, **13c**, **14c**, and **15c**) leads to a ca. 13 ppm upfield shift of C(7), while a downfield shift of ca. 3 ppm is observed for the corresponding chlorinated compounds (**3**, **13b**, **14b**, and **15b**). The assignments of C(1′) and C(4′) are based on the difference of the coupling constants ^1J(C, H), which are larger for C(1′) than for C(4′) (Table 2).[19]

pK_a Values and Tautomerism. The strength of the hydrogen bonds between nucleobases within a base pair depends on various parameters, including the pK_a values of the nucleobase moieties. Thus, it was conceivable to determine the pK_a values of compounds **2**−**4**. For this, UV-spectrophotometric titrations[20] were performed between pH 1.5−13.5 (Supporting Information). All three "isoguanine" nucleosides show two pK_a values (**2**: 4.6, 10.5; **3**: 3.9, 9.7; and **4**: 3.8, 9.8). From the data, it is apparent that the electron-withdrawing 7-halogeno substituents in **3** and **4** decrease the pK_a values significantly compared to that of the nonhalogenated compound **2**. This will affect the base-pair stability and also the prototropic equilibria.

In aqueous solution, the canonical DNA constituents (e.g., 2′-deoxyguanosine) exist predominantly in the keto (lactim) form, which leads to an almost perfect Watson−Crick base pairing ($K_{TAUT} \approx 10^4-10^5$).[21] As only one of 10^4-10^5 of the dG molecules is enolized, mispairing is low. Also, compound **1** exists mostly in the keto form, which can implement stable base pairs with dC or isoC_d. However, a significant amount of the enol tautomer is formed in this case (10% in water).[10] This allows the formation of stable mismatches with dT or dU and decreases the discrimination ability of isoguanine during base pairing (Figure 1).[11] Earlier, **2** was synthesized in our laboratory, and the N1−H, 2-keto form was identified in the solid state.[12b] Recently, it has been reported that this form is also favored in aqueous solution.[13] As the pK_a values of 7-halogenated nucleobases **3** and **4** are changing significantly, we assume that this will also influence the tautomeric equilibrium and might increase the population of the keto form. Therefore, the base discrimina-

(19) Seela, F.; Bussmann, W. *Nucleosides Nucleotides* **1985**, *4*, 391−394.
(20) Albert, A.; Serjeant, E. P. *The Determination of Ionization Constants*; Chapman and Hall: London, 1971; pp 44−64.
(21) Topal, M. D.; Fresco, J. R. *Nature* **1976**, *263*, 285−289.

Table 2. ^{13}C NMR Chemical Shifts (δ) of 7-Deaza-2′-deoxyisoguanosine Derivatives[a]

compd[b,c]	C(2)[d] C(2)	C(4)[d] C(6)	C(4a) C(5)	C(5) C(7)	C(6) C(8)	C(7a)[d] C(4)	C(1′)	C(2′)	C(3′)	C(4′)	C(5′)	HC=N	NMe_2	=CMe
2[12a]	153.9	156.3	92.6	100.8	118.9	152.6	83.4	*e*	71.1	87.2	62.0			
3[18a]	153.2	156.2	90.2	103.7	116.2	*f*	82.6	*e*	70.9	87.2	61.9			
4[18a]	153.6	156.0	91.0	87.4	118.8	*f*	82.5	*e*	70.8	87.2	61.8			
11	158.4	156.1	99.1	87.4	121.5	151.4	82.6	*e*	70.8	87.3	61.8			
12	154.8	152.7	109.0	89.1	126.5	152.4	82.9	*e*	70.8	87.7	61.7			
13a	157.1	156.4	98.2	101.0	121.7	155.3	82.7	*e*	71.1	87.1	62.1	161.5	38.5, 37.8	17.4
13b	156.2	156.0	95.7	104.4	118.4	155.8	82.3	*e*	71.0	87.2	62.0	161.3	38.4, 37.9	17.6
13c	156.2	156.0	96.6	88.6	120.9	*f*	82.3	*e*	71.0	87.2	61.9	160.9	38.3. 37.8	17.7
14a	162.5	155.4	109.3	100.7	123.4	151.7	82.8	*e*	71.0	87.3	62.0	161.5	38.3, 37.8	16.5
14b	162.3	156.0	105.7	104.8	120.5	150.6	82.8	*e*	71.0	87.5	61.9	161.8	38.4, 37.8	16.7
14c	162.1	155.7	106.7	89.0	122.9	150.9	82.7	*e*	70.9	87.4	61.8	161.5	38.4, 37.8	16.7
15a	162.6	155.6	109.2	101.0	122.9	151.9	82.2	*e*	70.8	85.5	64.1	161.7	*e*	16.5
15b	162.3	156.2	105.7	105.1	120.2	150.7	82.3	*e*	70.6	85.6	64.2	162.0	*e*	16.8
15c	162.3	156.0	106.8	89.4	122.6	151.1	82.4	*e*	70.7	85.6	64.2	161.7	*e*	16.8

[a] Measured in DMSO-d_6. [b] Systematic numbering. [c] Purine numbering. [d] Tentative. [e] Superimposed by DMSO. [f] Not detected.

Scheme 4. Tautomers of 7-Deazaisoguanosines **3** and **4**

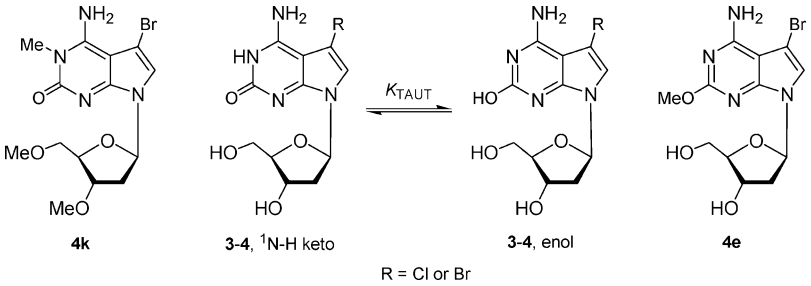

tion will increase, in particular against dT. For this purpose, the tautomeric equilibrium between the keto and the enol forms of **3** and **4** was determined UV-spectrophotometrically in aqueous and nonaqueous solution.

According to Figure 2A, the UV spectra of compounds **3** and **4**, measured in water, show the same maxima (306 and 261 nm), resembling the fixed keto form **4k** (Scheme 4). However, under nonaqueous conditions (100% dioxane), the UV absorbance changes totally, showing the maxima of the fixed enol form **4e** (265 and 281 nm) (Figure 2B). (The syntheses and analytical data of compounds **4k** and **4e** are described in the Supporting Information.) Therefore, it is reasonable to assume that in aqueous solution the halogenated derivative **3** or **4** exists almost entirely in the keto form, while in dioxane solution the enol form is the predominant species. Next, the tautomeric equilibria (K_{TAUT} = [keto]/[enol]) of compounds **3** and **4** were determined in a dioxane/water mixture ranging from 98:2 to 2:98. The ratio of the tautomers was determined by the multiwavelength method of Dewar and Urch.[22a] Data were collected at 281 and 306 nm, where the extinction coefficients of both forms show the highest difference (Figure 2). When the water/dioxane ratio was increased, the UV spectra for **3** and **4** shifted gradually, more and more resembling the UV spectra of the keto form. When the water content was higher than 25%, the UV spectra became solvent-

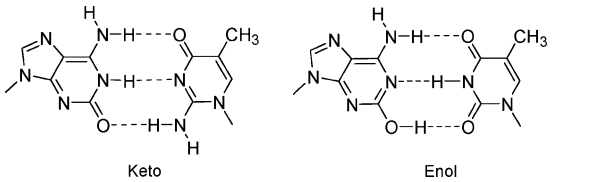

Figure 1. Keto and enol tautomers of isoguanine pair with isoC (or C) and T (or U).

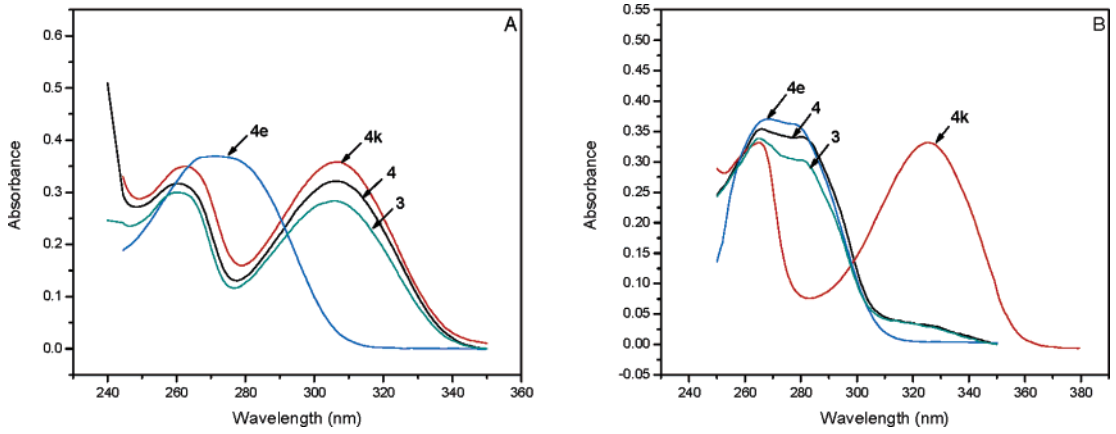

Figure 2. UV spectra of compounds **3**, **4**, **4k**, and **4e** in water (A) and in dioxane (B).

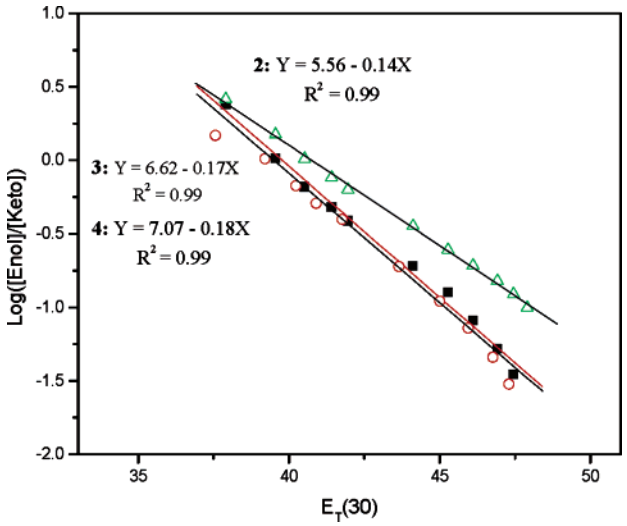

Figure 3. Plot of log([enol]/[keto]) versus $E_T(30)$ for compounds **2** (△), **3** (○), and **4** (■) in mixtures of dioxane ($E_T(30) = 36.0$) and water ($E_T(30) = 63.1$).

independent (Supporting Information) and the band at 281 nm nearly disappeared, while the absorbance at 306 nm increased to the level of the pure keto form. By adding more water, the whole spectrum is moved to shorter wavelength due to the increase of the polarity of the solvent mixture. The composition of keto and enol forms was maintained at the same level. From these data, the K_{TAUT} values were determined quantitatively by the methods of Shugar et al.[10] and Voegel et al.[22b] A plot of the logarithm of the tautomeric equilibrium constant for **3** and **4** versus the polarity parameter $E_T(30)$ of a set of the dioxane−water mixtures is shown in Figure 3. When the values of $E_T(30)$ are in the range of 38−50, the relationship between the log [K_{TAUT}] and the $E_T(30)$ is linear. This can be used to estimate the value of K_{TAUT} in aqueous solution. By extrapolating this linear relationship to the $E_T(30)$ value of water (63.1),[23] the tautomeric equilibrium constants for compounds **3** and **4** are estimated to be about 10^4.

For comparison, the K_{TAUT} of the parent nucleoside **2** was measured. The calculated value of K_{TAUT} for compound **2** was found to be about 2000 (Supporting Information), a value that agrees with that measured by Benner et al.[13] In conclusion, the population of the keto form of compound **3** or **4** in water is significantly higher than that of compound **2** and comes close to the value for naturally occurring 2′-deoxyguanosine ($K_{TAUT} \approx 10^4-10^5$).[21] Consequently, the halogenated nucleosides should increase the specificity to form a base pair with dC (parallel DNA) or iC_d (antiparallel DNA) over that of dT.

Next, a single-crystal X-ray analysis of compound **4** was performed. The crystal structure is characterized by the anti orientation around the *N*-glycosylic bond with the O4′−C1′−N9−C4 torsion angle of $\chi = -114.0°$ and the *S* conformation of pentofuranose moiety [the phase angle of pseudorotation: $P = 153.9°$ ($^2T_1 \rightleftarrows {}^2E$) and the puckering amplitude: $\psi_m = 43.6°$]. According to the bond length of C2−O2 [1.261(7) Å], it is apparent that the molecule adopts the 2-keto form.[12b] In addition,

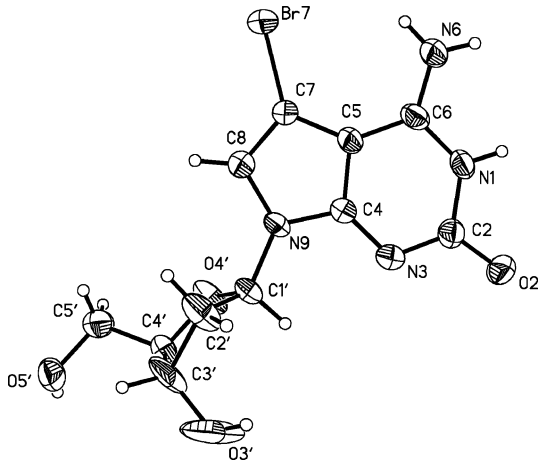

Figure 4. Crystal structure of compound **4**: the anti conformation of the base about the glycosylic bond [torsion angle χ (O4′−C1′−N9−C4) is −114.9°] and the *S* conformation of pentofuranose ring ($P = 153.9°$, $\psi_m = 43.6°$). The complete data of the structure will be published elsewhere.

the N1−C2 bond length is 0.077 Å longer than that of N3−C2 [1.335 (7) Å], which suggests that the ring proton is localized at N1. Obviously, in crystalline state the base ring adopts N1−H, 2-keto-6-amino tautomeric form, which is in line with the structure of compound **4** in aqueous solution (Figure 4) (Seela et al., manuscript in preparation). To prove the higher discriminatory potential of compounds **3** and **4** against dT and to stabilize duplexes by the properties of 7-halogeno substituents, a series of oligonucleotides were synthesized.

Oligonucleotides. Synthesis. Oligonucleotide synthesis was performed on solid phase in an ABI 392-08 synthesizer employing phosphoramidite chemistry.[24] Oligonucleotides were purified by reversed-phase HPLC. The nucleoside composition of oligomers was determined by MALDI-TOF spectrometry (see Table 8, experimental part) as well as by enzymatic analysis using snake venom phosphodiesterase followed by alkaline phosphatase. The mixture was analyzed on reversed-phase HPLC (RP-18) (see Figure 10, experimental part). The stability of oligonucleotide duplexes was determined by temperature-dependent UV measurements (Cary 1E, Varian) (see Experiment Section).

Base-Pairing Properties of the 7-Deaza-2′-deoxyisoguanosine Analogues 3 and 4. Recently, the base pairing of **1** and its 7-deazapurine derivatives has been investigated in our laboratory.[4c,12a,25] It was demonstrated that the 7-deazapurine nucleoside **2** was an effective substitute of ′**1** because of the high stability of the *N*-glycosylic bond,[26] accompanied by similar base-paring properties. Nevertheless, it was observed that both nucleosides showed base-pair ambiguity, in particular against dT.[12a,14b] Apparently, the higher keto form population of compound **2** (10^3) is not sufficient to result in a better discrimination among the cognate and noncognate bases. Now, much better base selectivity was expected due to the increased $K_{TAUT} \approx 10^4$ for the halogenated nucleosides **3** and **4**. Furthermore, the 7-halogeno substituent should be beneficial to the duplex stability as it was reported for related nucleo-

(22) (a) Dewar, M. J. S.; Urch, D. S. *J. Chem. Soc.* **1957**, 345−347. (b) Voegel, J. J.; von Krosigk, U.; Benner, S. A. *J. Org. Chem.* **1993**, *58*, 7542−7547.
(23) (a) Reichardt, C.; Harbusch-Görnert, E. *Liebigs Ann. Chem.* **1983**, 721−743. (b) von Jouanne, J.; Palmer, D. A.; Kelm, H. *Bull. Chem. Soc. Jpn.* **1978**, *51*, 463−465. (c) von Dimroth, K.; Reichardt, C.; Siepmann, T.; Bohlmann, F. *Liebigs Ann. Chem.* **1963**, *661*, 1−37.
(24) *Users' Manual of the DNA Synthesizer*; Applied Biosystems: Weiterstadt, Germany, p 392.
(25) Seela, F.; Kröschel, R. *Nucleic Acids Res.* **2003**, *31*, 7150−7158.
(26) Seela, F.; Menkhoff, S.; Behrendt, S. *J. Chem. Soc., Perkin Trans. II* **1986**, 525−530.

Table 3. T_m Values and Thermodynamic Data for ps-Oligonucleotides with Alternating Bases[a]

duplex	T_m (°C)	ΔT_m[b] (°C)	duplex	T_m (°C)	ΔT_m[b] (°C)
5′-d(**1**−C−**1**−C−**1**−C) (**16**)[c]	33		5′-d(**1**−T)$_6$ (**20**)	46	
5′-d(**1**−C−**1**−C−**1**−C) (**16**)			5′-d(C−A)$_6$ (**21**)		
5′-d(**2**−C−**2**−C−**2**−C) (**17**)[c]	22	−2.2	5′-d(**2**−T)$_6$ (**22**)	47	
5′-d(**2**−C−**2**−C−**2**−C) (**17**)			5′-d(C−A)$_6$ (**21**)		
5′-d(**3**−C−**3**−C−**3**−C) (**18**)	54	+4.2	5′-d(**3**−T)$_6$ (**23**)	59	+2.2
5′-d(**3**−C−**3**−C−**3**−C) (**18**)			5′-d(C−A)$_6$ (**21**)		
5′-d(**4**−C−**4**−C−**4**−C) (**19**)	56	+4.6	5′-d(**4**−T)$_6$ (**24**)	60	+2.3
5′-d(**4**−C−**4**−C−**4**−C) (**19**)			5′-d(C−A)$_6$ (**21**)		
			5′-d(**G**−T)$_6$ (**25**)	56	
			3′-d(C−A)$_6$ (**26**)		

[a] Measured in 1.0 M NaCl, 0.1 M $MgCl_2$, and 60 mM Na-cacodylate buffer, pH 7.0, with 5 μM + 5 μM single-strand concentration. [b] T_m increase per modification. [c] See Seela et al.[14a]

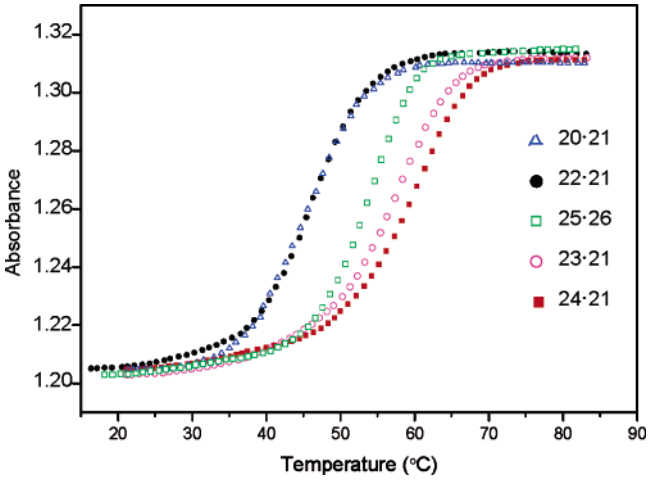

Figure 5. T_m profiles of ps-duplexes containing compounds **1**−**4** and the corresponding aps-DNA. Measured in 1.0 M NaCl, 0.1 M $MgCl_2$, and 60 mM Na-cacodylate buffer, pH 7.0, with 5 μM + 5 μM single-strand concentration.

sides.[16,25] Consequently, compounds **3** and **4** were incorporated in oligonucleotide duplexes with ps and aps chain orientation, and their base-pair stability and base selectivity were studied.

Self-Complementary and Non-Self-Complementary ps-Duplexes with Alternating Base Composition. The self-complementary hexanucleotide 5′-d(**2**−C)$_3$ (**17**) forms a ps-duplex with two nucleoside overhangs, which was found to be less stable than the purine counterpart 5′-d(**1**−C)$_3$ (**16**).[14a] Now, the halogenated duplexes 5′-d(**3**−C)$_3$ (**18·18**) and 5′-d(**4**−C)$_3$ (**19·19**), incorporating 7-chloro- (**3**) or 7-bromo derivative (**4**) of nucleoside **2**, were investigated. From the data given in Table 3, it is apparent that compounds **3** and **4** strongly increase duplex stability. Their stabilizing effect amounts to +4.2 °C per modification for compound **3** and +4.6 °C for **4**. Compared to the nonhalogenated compound **2** with ΔT_m = −2.2 °C per modification (duplex **17**), the incorporation of nucleosides **3** and **4** results in a T_m increase of 6−7 °C per modification.

Next, the effect of compounds **3** and **4** on non-self-complementary duplexes with alternating bases such as 5′-d(iGT)$_6$·5′-d(CA)$_6$ was studied. These duplexes do not form overhangs, and their stability can be directly compared with their antiparallel stranded counterparts. Figure 5 shows T_m profiles of ps-duplexes containing compounds **1**−**4** and the corresponding aps-DNA. It can be seen that aps-duplex **25·26** shows high cooperativity during the melting, indicated by a narrow range of the melting profile. Although the ps-duplexes **23·21** and **24·21** showed a somewhat broader melting range, it is evident that the T_m values of ps-duplex containing **3** or **4** are significantly higher than those of the corresponding ps-duplexes **20·21** and **22·21**. The ps-duplexes incorporating the **3**−dC or **4**−dC base pairs (**23·21**: T_m = 59 °C and **24·21**: T_m = for 60 °C) were ∼3−4 °C more stable than the corresponding aps-duplex **25·26** containing dG−dC base pairs (T_m = 56 °C) (Table 3). Apparently, the 7-halogeno substituents stabilize the "isoG_d−dC" pair strongly compared to the nonfunctionalized nucleosides **1** or **2** in ps-duplexes **20·21** (46 °C) or **22·21** (47 °C) (Figure 5). This stability increase makes parallel DNA as equally stable as aps-DNA containing the canonical dG−dC base pairs. The smaller stabilization found in these series of oligonucleotide duplexes compared to the self-complementary ones results from the fact that the latter are further stabilized by the base stacking of the 5′ overhangs.[27] As the self-complementary duplexes of Table 3 are formed by only five base pairs compared to six pairs in the series of the non-self-complementary duplexes, the contribution of the overhangs is higher than that of one base pair.

Parallel-Stranded Duplexes with Random Base Composition. Apart from self-complementary and non-self-complementary ps-duplexes with alternating base composition, ps-duplexes with random base composition were investigated next (Table 4). To induce parallel chain orientation, particular sequence motifs were chosen and dG−dC base pairs were replaced by "iG_d"−dC or ^{Me}iC_d−dG pairs. The role of 7-halogeno substituents was studied on two different duplex series, namely **27·28** and **32·33**, both incorporating two modified nucleosides **3** or **4** in place of iG_d opposite to dC. In the first series of duplexes, the modified nucleosides were arranged in a consecutive order while in the second the modification sites were separated.

As shown in Table 4, both nucleosides **3** and **4** increase the duplex stability significantly, while nucleoside **2** shows base-pair stability almost as identical as those containing **1**. Although the stability of these two duplexes are dependent on the position of incorporation (T_m = 44 °C for **27·28** and T_m = 39 °C for **32·33**), the T_m enhancement of 7-halogenated derivatives containing duplexes is in the same range with a ΔT_m = +2.0 °C per modification for **3** (duplexes **30·28** and **35·33)** and +2.5 °C for **4** (duplexes **31·28** and **36·33**). These stabilizing effects are identical to those in non-self-complementary alternating duplexes, which shows that the nearest-neighbor stacking does not affect the stabilizing effect of compound **3** or **4** on these parallel stranded duplexes.

(27) Rosemeyer, H.; Seela, F. *J. Chem. Soc., Perkin Trans. II* **2002**, 746−750.

Table 4. T_m Values and Thermodynamic Data of ps-Duplexes with Random Base Composition[a,b]

duplex	T_m (°C)	ΔT_m[c] (°C)	duplex	T_m (°C)	ΔT_m[c] (°C)
5′-d(TiCATAAiCT**11**AT) (**27**)[d]	44		5′-d(ATiCiCA**1**TTAT**1**A) (**32**)[d]	39	
5′-d(AGTATTGACCTA) (**28**)			5′-d(TAGGTCAATACT) (**33**)		
5′-d(TiCATAAiCT**22**AT) (**29**)[d]	44	0	5′-d(ATiCiCA**2**TTAT**2**A) (**34**)[d]	39	0
5′-d(AGTATTGACCTA) (**28**)			5′-d(TAGGTCAATACT) (**33**)		
5′-d(TiCATAAiCT**33**AT) (**30**)	48	+2.0	5′-d(ATiCiCA**3**TTAT**3**A) (**35**)	43	+2.0
5′-d(AGTATTGACCTA) (**28**)			5′-d(TAGGTCAATACT) (**33**)		
5′-d(TiCATAAiCT**44**AT) (**31**)	49	+2.5	5′-d(ATiCiCA**4**TTAT**4**A) (**36**)	44	+2.5
5′-d(AGTATTGACCTA) (**28**)			5′-d(TAGGTCAATACT) (**33**)		

[a] Measured in 1.0 M NaCl, 0.1 M $MgCl_2$, and 60 mM Na-cacodylate buffer, pH 7.0, with 5 μM + 5 μM single-strand concentration. [b] d(iC) = $^{Me}iC_d$ = 5-methyl-2′-deoxyisocytidine. [c] T_m increase per modification. [d] See Seela et al.[12a]

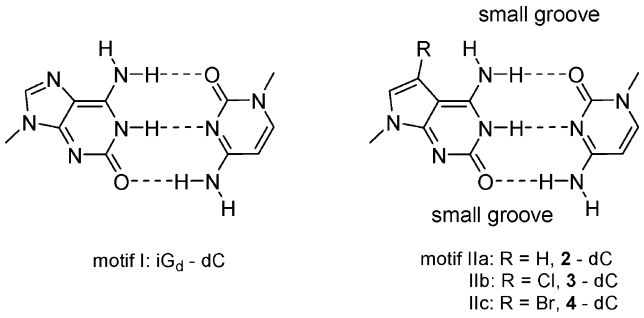

Figure 6. "iG$_d$−dC" base-pair motifs in duplexes with parallel chain orientation.

Figure 6 shows the base-pair motifs of the duplexes with parallel chain orientation. Analogously to the base-pair motif I of iG$_d$−dC, motifs IIa−c are suggested for the "c^{7}iG$_d$"−dC pair. A significant stabilization of the duplex structure by incorporation of 7-halogenated nucleoside **3** or **4** instead of **2** can be attributed to (i) a hydrophobization of the small groove, (ii) increased stacking interaction of the modified base, and (iii) better proton donor properties of H−N(1) causing stronger hydrogen bonding within the base pairs. In the case of compounds **3** and **4**, on the one hand, the introduction of 7-halogeno substituents increases the hydrophobic properties of the modified bases, on the other hand increases the polarizabilities ($\alpha_m/10^{-24}$ cm^3) of the nucleobases (14.83 for **2**, 16.85 for **3**, and 17.55 for **4**, calculated by Hyperchem 7.0). Accordingly, the stacking interaction was increased. Furthermore, better proton donor properties of H−N(1) causing stronger hydrogen bonding within the base pairs play an important role in the stability of **3**−dC or **4**−dC base pairs. This is underlined by the pK_a values of deprotonation (**2**: 10.5; **3**: 9.7; **4**: 9.8). Consequently, compounds **3** and **4** are stronger proton donors in the base pairs of **3**−dC (IIb) or **4**−dC (IIc) pairs compared to that of **2**−dC (IIa).

Duplexes with Antiparallel Chain Orientation. As shown in Table 5, aps-duplexes containing **1**−$^{Me}iC_d$ base pairs are more stable than those containing dG−dC pairs (see duplexes **37·38**, **27·32**, **33·28**, and **33a·28a**), an observation that has been already reported.[12a] According to Table 5, it is also apparent that the stability of the iG$_d$−$^{Me}iC_d$ base pair is increased when iG$_d$ (**1**) is replaced by compound **3** or **4**. The duplexes with one incorporation of **3** or **4** opposite to $^{Me}iC_d$ (T_m = 57 °C for both **37·40** and **37·41**) show T_m values 3 °C higher than that of the parent duplex **37·38** (T_m = 54 °C) or that containing **2** (**37·39**, T_m = 54 °C) (Table 5). Incorporation of four modified base pairs showed a T_m increase of 7 °C for duplex **30·35** and 8 °C for **31·36** (Table 5). Both 7-halogenated nucleosides cause very similar stabilization. A related base-pair motif as reported for iG$_d$−$^{Me}iC_d$ (motif III) or **2**−$^{Me}iC_d$ pair (motif IVa) is also suggested for that of the 7-deazapurine nucleosides **3** and **4** (motifs IVb,c) (Figure 7).

Mismatch Discrimination. The hybridization experiments of iG$_d$ toward four canonical nucleosides in vitro have been investigated by Seela et al.[12a] and Kawakami et al.[14b] using iG$_d$−iC$_d$ or dA−dT base pair as the control. It was found that iG$_d$ forms similar stable base pairs with dT, dC, and dG but not with dA when the base pair was located in the center of the sequences. If the duplexes contain the mismatch base pairs at the end, the stability of duplexes was dependent on the sequences.[14b] Nevertheless, the thermodynamic stabilities of mismatch base pairs were in agreement with the tendency of the mutagenic misincorporation of the nucleosides opposite to iG$_d$ in vitro, suggesting that the thermodynamic stability of the base pairs may be an important factor for the mutation spectra of iG$_d$.[14b] Among the mismatches of iG$_d$ toward dC, dG, and dT during the vitro replication, the most serious problem is the misincorporation of iG$_d$ opposite dT in the DNA template.[5a,7,8] This might result from the enol tautomer of isoguanine nucleosides existing in aqueous solution to a significant amount (10%).[10]

As discussed above, the enol population is significantly decreased in the case of the halogenated 7-deaza-2′-deoxyisoguanosines **3** and **4** compared to their nonhalogenated counterparts. Now, we are investigating oligonucleotide duplexes containing the nucleosides **1**−**4** located opposite the four canonical nucleosides. These studies include duplexes with parallel as well as with antiparallel chain orientation. Table 6 summarizes the data for ps-oligonucleotides containing base pairs with **1**, **2**, as well as those incorporating compound **3** or **4** in a position opposite the four canonical nucleosides. From the data, it is apparent that the most stable base pairs formed in all cases are those with dC, while those incorporating mismatches show comparable T_m decreases. The two series of oligonucleotide duplexes containing the modifications at different positions show that the mismatch discrimination is position-dependent. As expected, a stronger discriminatory effect occurs when the modification is in the middle of the duplexes (**35·37** and **36·37**), while it is less pronounced near the termini (duplexes **30·45** and **31·45**), which was also observed in the case of **1** and **2** (Table 6). The most striking result of this investigation is the finding that the base discrimination of the halogenated nucleosides **3** and **4** is superior to that of the nonfunctionalized nucleosides **1** and **2**. In particular, the base pair of compounds **3** and **4** with dT shows a significantly enhanced base discrimination (higher ΔT_m values).

Table 5. T_m Values and Thermodynamic Data of aps-Duplexes with Random Base Composition[a,b]

duplex	T_m (°C)	ΔT_m[c] (°C)	duplex	T_m (°C)	ΔT_m[c] (°C)
5′-d(TAGGTCAATACT) (**33**) 3′-d(ATCCAGTTATGA) (**28**)	51		3′-d(TAGGTCAATACT) (**33a**) 5′-d(ATCCAGTTATGA) (**28a**)	49	
5′-d(TAGGT**iC**AATACT) (**37**) 3′-d(ATCCA**1**TTATGA) (**38**)	54		3′-d(TA**11**TiCAATAiCT) (**27**)[d] 5′-d(ATiCiCA**1**TTAT**1**A) (**32**)	60	
5′-d(TAGGT**iC**AATACT) (**37**) 3′-d(ATCCA**2**TTATGA) (**39**)	54	0	3′-d(TA**33**TiCAATAiCT) (**30**) 5′-d(ATiCiCA**3**TTAT**3**A) (**35**)	67	+1.8
5′-d(TAGGT**iC**AATACT) (**37**) 3′-d(ATCCA**3**TTATGA) (**40**)	57	+3.0	3′-d(TA**44**TiCAATAiCT) (**31**) 5′-d(ATiCiCA**4**TTAT**4**A) (**36**)	68	+2.0
5′-d(TAGGT**iC**AATACT) (**37**) 3′-d(ATCCA**4**TTATGA) (**41**)	57	+3.0			

[a] Measured in 1.0 M NaCl, 0.1 M $MgCl_2$, and 60 mM Na-cacodylate buffer, pH 7.0, with 5 μM + 5 μM single-strand concentration. [b] d(iC) = $^{Me}iC_d$ = 5-methyl-2′-deoxyisocytidine. [c] T_m increase per modification. [d] See Seela et al.[12a]

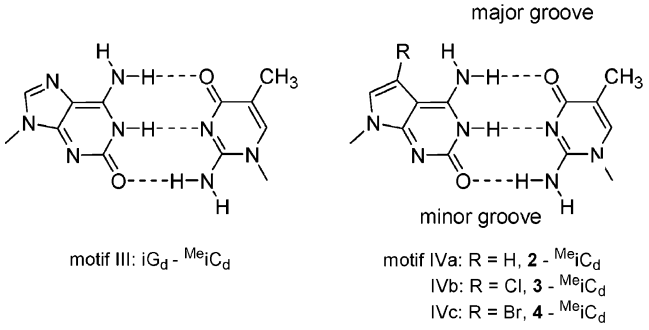

Figure 7. "iG_d−iC_d" base-pair motifs in duplexes with antiparallel chain orientation.

Table 6. T_m Values and Thermodynamic Data of ps-Duplexes with Mismatches Opposite to **1**−**4**[a]

	5′-d(TiCATAAiCT**X**XAT)-3′[b] 5′-d(AG TATT GA**Y**CTA)-3′			5′-d(ATiCiCA**X**TTATXA)-3′[b] 5′-d(TA G GT**Y**AATACT)-3′		
X·Y	duplex	T_m (°C)	ΔT_m[c] (°C)	duplex	T_m (°C)	ΔT_m[c] (°C)
1·C[d]	**27·28**	44		**32·33**	39	
1·G[d]	**27·42**	36	−8	**32·46**	−	−
1·T[d]	**27·43**	33	−11	**32·47**	31	−8
1·A[d]	**27·44**	34	−10	**32·48**	34	−5
1·iC[b,d]	**27·45**	40	−4	**32·37**	30	−9
2·C[d]	**29·28**	44		**34·33**	39	
2·G[d]	**29·42**	33	−11	**34·46**	−	−
2·T[d]	**29·43**	31	−13	**34·47**	29	−10
2·A[d]	**29·44**	32	−12	**34·48**	29	−10
2·iC[b,d]	**29·45**	37	−7	**34·37**	−	−
3·C	**30·28**	48		**35·33**	43	
3·G	**30·42**	34	−14	**35·46**	−	−
3·T	**30·43**	31	−17	**35·47**	28	−15
3·A	**30·44**	31	−17	**35·48**	30	−13
3·iC	**30·45**[c]	44	−4	**35·37**	36	−7
4·C	**31·28**	49		**36·33**	44	
4·G	**31·42**	36	−13	**36·46**	−	−
4·T	**31·43**	31	−18	**36·47**	29	−15
4·A	**31·44**	31	−18	**36·48**	28	−16
4·iC	**31·45**	45	−4	**36·37**[c]	36	−8

[a] Measured in 1.0 M NaCl, 0.1 M $MgCl_2$, and 60 mM Na-cacodylate buffer, pH 7.0, with 5 μM + 5 μM single-strand concentration. [b] d(iC) = $^{Me}iC_d$ = 5-methyl-2′-deoxyisocytidine. [c] $\Delta T_m = T_m^{\text{base match}} - T_m^{\text{base match}}$. [d] See Seela et al.[12a]

Next, duplexes with antiparallel chain orientation were investigated. As listed in Table 7, the **3**−$^{Me}iC_d$ and **4**−$^{Me}iC_d$ are the most stable base pairs as indicated from the highest T_m of the corresponding duplexes, while **3** or **4** located opposite to dC, dG, dA, or dT reduce duplex stability with the least stable duplex for the "iG_d"−dA pair. It can be further seen that compounds **3** and **4** are much more discriminatory against mispair formation than the nonfunctionalized nucleosides **1** and **2**. The stability of duplexes incorporating "iG_d"−dT or "iG_d"−dA increased in the order: **3** ≈ **4** < **1** ≈ **2**. This can be clearly seen from Figure 8A−D. According to Figure 8C,D, it is apparent that compounds **3** and **4** show much stronger discrimination with dA or dT than compounds **1** and **2** (Figure 8A,B) as indicated by the order of $|\Delta T_m|$ (**1** ≈ **2** < **3** ≈ **4**).

Table 7. T_m Values and Thermodynamic Data of aps-Duplexes with Mismatches Opposite to **1**−**4**[a]

	5′-d(TAGGT**X**AATACT)-3′ 3′-d(ATCCA**Y**TTATGA)-5′			5′-d(AGTATTGA**X**CTA)-3′ 3′-d(TCATAACT**Y**GAT)-5′		
X·Y	duplex	T_m (°C)	ΔT_m[b] (°C)	duplex	T_m (°C)	ΔT_m[b] (°C)
iC·1[c,d]	**37·38**	54		**45·49**	54	
C·1[d]	**33·38**	44	−10	**28·49**	44	−10
G·1[d]	**46·38**	44	−10	**42·49**	44	−10
T·1[d]	**47·38**	42	−12	**43·49**	45	−9
A·1[c,d]	**48·38**	32	−22	**44·49**	35	−19
iC·2[c,d]	**37·39**	54	0	**45·50**	52	
C·2[d]	**33·39**	43	−11	**28·50**	43	−9
G·2[d]	**46·39**	42	−12	**42·50**	44	−8
T·2[d]	**47·39**	42	−12	**43·50**	44	−8
A·2[d]	**48·39**	29	−25	**44·50**	31	−21
iC·3[c]	**37·40**	57		**45·51**	56	
C·3	**33·40**	47	−10.0	**28·51**	48	−8.0
G·3	**46·40**	44	−13.0	**42·51**	45	−11.0
T·3	**47·40**	40	−17.0	**43·51**	43	−13.0
A·3	**48·40**	28	−29.0	**44·51**	29	−27.0
iC·4[c]	**37·41**	57		**45·52**	56	
C·4	**33·41**	47	−10.0	**28·52**	47	−9.0
G·4	**46·41**	45	−12.0	**42·52**	45	−11.0
T·4	**47·41**	40	−17.0	**43·52**	43	−13.0
A·4	**48·41**	27	−30.0	**44·52**	33	−23.0

[a] Measured in 1.0 M NaCl, 0.1 M $MgCl_2$, and 60 mM Na-cacodylate buffer, pH 7.0, with 5 μM + 5 μM single-strand concentration. [b] $\Delta T_m = T_m^{\text{base mismatch}} - T_m^{\text{base match}}$. [c] d(iC) = $^{Me}iC_d$ = 5-methyl-2′-deoxyisocytidine. [d] See Seela et al.[12a]

Regarding the various base-pair motifs formed by mispairing in duplexes with parallel or antiparallel chain orientation, the enol tautomer of **1** is responsible for two major mismatches (Figure 9). A stable tridentate mispair of **1** with dT is formed in the parallel duplexes according to motif V, while motif VI causes the mispairing in antiparallel DNA.[5a,11,12a] These motifs are likely to be formed also in the case of **2**. Apparently, the $K_{TAUT} \approx 10^3$ of compound **2** is not sufficient to suppress mispairing. On the contrary, the halogenated compounds **3** and **4** ($K_{TAUT} \approx 10^4$) are not able to form such a mispair, at least not to a significant extent due to the low content of the enol form. Another mismatch formed in parallel DNA, which results from the relatively high T_m values shown in Table 6, is that between $isoG_d$ or 7-deaza-2′-deoxyisoG and iC_d. The likely base-pair motif in this case is VII. A corresponding base pair between $isoG_d$ and dC as shown in the motif X seems to be of minor importance in the aps-duplexes according to the ΔT_m

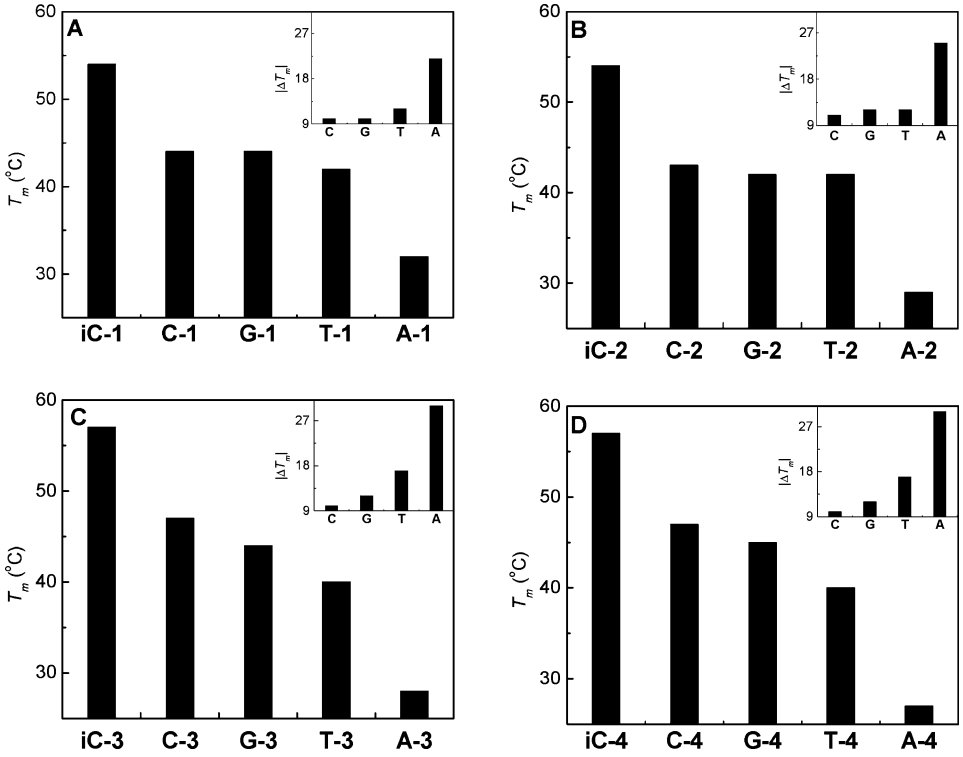

Figure 8. Graphs showing the stability of oligonucleotide duplexes containing mismatches with compounds **1**−**4** opposite to isoC$_d$, dC, dG, dT, and dA. The insets show the $|\Delta T_m|$ of $T_m^{\text{base mismatch}} - T_m^{\text{base match}}$ for the evaluation of the discriminatory effects.

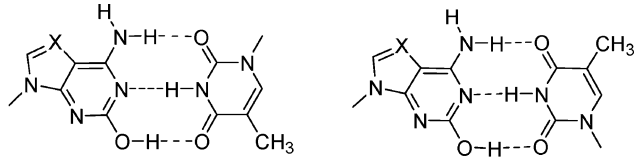

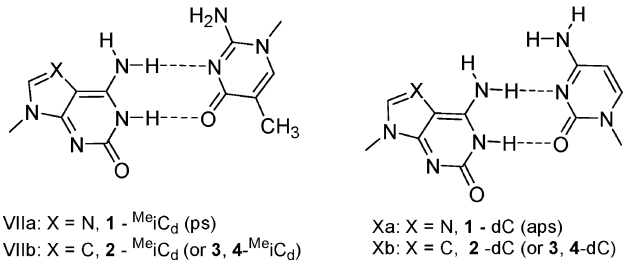

Figure 9. Odd base-pairs motifs related to "iG$_d$−iC$_d$" (ps), "iG$_d$−dT"-(ps), "iG$_d$−dC" (aps), and "iG$_d$−dT" (aps).

values shown in Table 7. These results reveal that, from the viewpoint of thermodynamic stability, compounds **3** and **4** reduce the mispairing during hybridization, a phenomenon that should also minimize the chance of mispair formation of dT opposite to iG$_d$ in DNA replication.

Conclusion

Oligonucleotides containing **2** or 7-halogenated derivatives (**3** and **4**) are synthesized using the phosphoramidites **5**−**7**. No particular oxidation conditions are required during solid-phase synthesis as recommended for oligonucleotides containing 7-deaza-2′-deoxyguanosine. Compared to the purine nucleoside **1**, the stability of the base pairs of the halogenated compound **3** or **4** with 2′-deoxy-5-methylisocytidine is significantly increased in antiparallel DNA or with dC in parallel DNA. Moreover, the base discrimination against the four canonical DNA constituents, in particular against adenine and thymine, is significantly improved. This is underlined by the favored keto tautomer population of compounds **3** and **4** in aqueous solution compared to the nonhalogenated nucleosides **1** or **2**. Also, low glycosylic bond stability of compound **1** compared to that of the canonical nucleosides (acidic conditions) was overcome.

Earlier, it was reported that triphosphates of 7-halogenated or 7-alkynylated 7-deaza-2′-deoxyguanosines show good acceptance by various DNA polymerases.[28] Considering the favorable properties of 7-deazapurine 2′-deoxyribonucleosides, it is expected that the triphosphates of compounds **3** and **4** are good substrates as well-forming DNA fragments with antiparallel chain orientation. Also, a higher accuracy of nucleotide incorporation is expected for the triphosphates of **3** and **4** compared to those of **1** or **2**. Similarly, the ribonucleosides related to the structure of **3** or **4** or other 7-functionalized 7-deazaisoguanine nucleosides with 7-substituents of moderate size (e.g., propynyl residues) should show similar favorable properties compared to those containing a purine skeleton. Work in this area is now in progress.

Experimental Section

Materials. All chemicals were purchased from Sigma-Aldrich (Sigma-Aldrich Chemie GmbH, Taufkirchen, Germany). Solvents were of laboratory grade. Snake venom phosphodiesterase (EC 3.1.15.1, *Crotallus adamanteus*) and alkaline phosphatase (EC 3.1.3.1, *Escherichia coli*) were generous gifts from Roche Diagnostics GmbH, Germany. The synthesis of **2**, **3**, and **4** has been previously published.[12a,18]

(28) (a) Seela, F.; Feiling, E.; Gross, J.; Hillenkamp, F.; Ramzaeva, N.; Rosemeyer, H.; Zulauf, M. *J. Biotechnol.* **2001**, *86*, 269−279. (b) Augustin, M. A.; Ankenbauer, W.; Angerer, B. *J. Biotechnol.* **2001**, *86*, 289−301.

Procedures (Organic Synthesis). General. Thin-layer chromatography (TLC) was performed on TLC aluminum sheets covered with silica gel 60 F_{254} (0.2 mm, VWR International, Darmstadt, Germany). Column flash chromatography (FC): silica gel 60 (VWR International, Darmstadt, Germany) at 0.4 bar. UV spectra were recorded on a U-3200 spectrophotometer (Hitachi, Japan). NMR spectra were measured on an Avance-250 or AMX-500 spectrometers (Bruker, Rheinstetten, Germany). Chemical shifts (δ) are in ppm relative to internal Me_4Si or external H_3PO_4 (^{31}P). The *J* values are given in hertz. Elemental analyses were performed by the Mikroanalytisches Laboratorium Beller, Göttingen, Germany.

4-Amino-5-bromo-7-(2-deoxy-β-D-*erythro*-pentofuranosyl)-2-[(diphenylcarbamoyl)oxy]-7*H*-pyrrolo[2,3-*d*]pyrimidine (11). To a suspension of compound **4** (280 mg, 0.81 mmol) in dry pyridine (3.0 mL), diphenylcarbamoyl chloride (254 mg, 1.10 mmol) and *N*,*N*-diisopropylethylamine (0.2 mL, 1.15 mmol) were added and stirred for 2 h at room temperature. Then, the mixture was poured into 5% aqueous $NaHCO_3$ (10 mL) and extracted with CH_2Cl_2 (3 × 10 mL). The CH_2Cl_2 layers were combined, dried over Na_2SO_4, and filtered. After evaporation of the solvent, the residue was applied to FC (silica gel, column 3 × 10 cm). Elution with CH_2Cl_2 followed by CH_2Cl_2/MeOH (95:5 to 9:1) gave **11** as a colorless foam (340 mg, 78%). TLC (silica gel, 9:1 CH_2Cl_2/MeOH) R_f 0.43; UV λ_{max} (MeOH)/nm (ϵ/dm^3 mol^{-1} cm^{-1}): 276 (12 100), 230 (30 400); ^{1}H NMR (DMSO-d_6, 500 MHz): δ 2.12−2.19, 2.37−2.46 [2H, m, H_2−C(2′)], 3.44−3.58 [2H, m, H_2−C(5′)], 3.80−3.81 [1H, m, H−C(4′)], 4.31−4.33 [1H, 't', *J* = 3.8 Hz, H−C(3′)], 4.98 [1H, 't', *J* = 3.8 Hz, HO−C(5′)], 5.30 [1H, d, *J* = 3.9 Hz, HO−C(3′)], 6.39 [1H, 't', *J* = 7.6 Hz, H−C(1′)], 7.32−7.46 (12H, m, NH_2, arom. H,), 7.62 [1H, s, H−C(6)]; Anal. Calcd for $C_{24}H_{22}BrN_5O_5$ (540.4): C 53.34, H 4.10, N 12.96; found: C 53.40, H 4.20, N 12.82.

5-Bromo-7-(2-deoxy-β-D-*erythro*-pentofuranosyl)-4-[(2-methylpropanoyl)amino]-2-[(diphenylcarbamoyl)oxy]-7*H*-pyrrolo[2,3-*d*]-pyrimidine (12). To a solution of **11** (260 mg, 0.48 mmol) in dry pyridine (3.0 mL), chlorotrimethylsilane (0.2 mL, 1.58 mmol) was added. After the mixture was stirred for 30 min, isobutyryl chloride (0.16 mL, 1.53 mmol) was introduced and the stirring was continued for 4 h. The mixture was cooled in an ice bath. Upon addition of H_2O (1.0 mL), three portions of 25% NH_3/H_2O (3 mL) were added within 5 h under stirring in the ice bath. The mixture was poured into 5% aqueous $NaHCO_3$ (10 mL) and extracted with CH_2Cl_2 (3 × 10 mL). The CH_2Cl_2 layers were combined, dried over Na_2SO_4, and filtered. After evaporation of the solvent, the residue was submitted to FC (silica gel, column 3 × 10 cm). Elution with CH_2Cl_2 followed by CH_2Cl_2/MeOH (98:2 to 95:5) gave **12** as a colorless foam (29 mg, 10%). (Starting material **11** (200 mg) was recovered.) TLC (silica gel, 9:1 CH_2Cl_2/MeOH) R_f 0.51; ^{1}H NMR (DMSO-d_6, 500 MHz): δ 1.15, 1.17 [6H, 2s, CH(CH_3)$_2$], 2.23−2.26, 2.70−2.78 [2H, 2m, H_2−C(2′)], 3.50−3.56 [2H, m, H_2−C(5′)], 3.80−3.84 [1H, m, H−C(4′)], 4.31−4.35 [1H, m, H−C(3′)], 4.99 [1H, 't', *J* = 3.8 Hz, HO−C(5′)], 5.34 [1H, d, *J* = 3.8 Hz, HO−C(3′)], 6.54 [1H, 't', *J* = 6.1 Hz, H−C(1′)], 7.32−7.46 (10H, m, arom. H), 7.98 [1H, s, H−C(6)], 10.52 (1H, br. s, NH); Anal. Calcd for $C_{28}H_{28}BrN_5O_6$ (610.5): C 55.09, H 4.62, N 11.47; found: C 54.92, H 4.62, N 11.51.

7-(2-Deoxy-β-D-*erythro*-pentofuranosyl)-4-[(dimethylaminoethylidene)amino]-7*H*-pyrrolo[2,3-*d*]pyrimidine-2-one (13a). General Procedure for the Preparation of 13a−c. A suspension of **2** (266 mg, 1.0 mmol) in MeOH (10.0 mL) was stirred with *N*,*N*-dimethylacetamide dimethyl acetal (0.5 mL, 3.42 mmol) for 30 min at room temperature. After evaporation, the residue was applied to FC (silica gel, column 4 × 10 cm, elution with CH_2Cl_2/MeOH, 95:5 to 9:1), yielding **13a** as a colorless foam (305 mg, 91%); TLC (silica gel, 5:1 CH_2Cl_2/MeOH) R_f 0.54; UV λ_{max} (MeOH)/nm (ϵ/dm^3 mol^{-1} cm^{-1}): 231 (26 100); 264 (11 300); 341 (12 700); ^{1}H NMR (DMSO-d_6, 250 MHz): δ 2.04−2.06 [4H, m, (CH_3)$_2$N(CH_3)C═, H−C(2′)], 2.37−2.38 [1H, 1m, H−C(2′)], 3.06, 3.09 [6H, 2s, N(CH_3)$_2$], 3.50−3.51 [2H, m, H_2−C(5′)], 3.77−3.78 [1H, m, H−C(4′)], 4.27−4.28 [1H, m, H−C(3′)], 5.20 [2H, br. s, HO−(5′), HO−C(3′)], 6.06 [1H, d, *J* = 5.6 Hz, H−C(5)], 6.25−6.26 [1H, m, H−C(1′)], 7.02 [1H, d, *J* = 5.6 Hz, H−C(6)], 10.82 (1H, br. S, NH); Anal. Calcd for $C_{15}H_{21}N_5O_4$ (335.4): C 53.72, H 6.31, N 20.88; found: C 53.86, H 6.28, N 20.72.

5-Chloro-7-(2-deoxy-β-D-*erythro*-pentofuranosyl)-4-[(dimethylaminoethylidene)amino]-7*H*-pyrrolo[2,3-*d*]pyrimidine-2-one (13b). Compound **3** (301 mg, 1.0 mmol) was used, and **13b** was obtained as a colorless foam (333 mg, 90%); TLC (silica gel, 5:1 CH_2Cl_2/MeOH) R_f 0.57; UV λ_{max} (MeOH)/nm (ϵ/dm^3 mol^{-1} cm^{-1}): 238 (24 400); 268 (9400); 341 (10 700); ^{1}H NMR (DMSO-d_6, 500 MHz): δ 2.03−2.06 [4H, m, (CH_3)$_2$N(CH_3)C═, H−C(2′)], 2.28−2.37 [1H, 1m, H−C(2′)], 3.04, 3.10 [6H, 2s, N(CH_3)$_2$], 3.43−3.47 [2H, m, H_2−C(5′)], 3.75−3.78 [1H, m, H−C(4′)], 4.25−4.27 [1H, m, H−C(3′)], 5.08 [1H, br. s, HO−C(5′)], 5.26 [1H, d, *J* = 3.9 Hz, HO−C(3′)], 6.27 [1H, 't', *J* = 6.2 Hz, H−C(1′)], 7.17 [1H, s, H−C(6)], 10.98 (1H, br. S, NH); Anal. Calcd for $C_{15}H_{20}ClN_5O_4$ (369.8): C 48.72, H 5.45, N 18.94; found: C 48.80, H 5.55, N 18.79.

5-Bromo-7-(2-deoxy-β-D-*erythro*-pentofuranosyl)-4-[(dimethylaminoethylidene)amino]-7*H*-pyrrolo[2,3-*d*]pyrimidine-2-one (13c). Methods as described for **13a**, with **4** (500 mg, 1.45 mmol) in MeOH (20 mL) and *N*,*N*-dimethylacetamide dimethyl acetal (1.0 mL, 6.84 mmol). FC (silica gel, column 4 × 10 cm, elution with CH_2Cl_2/MeOH, 95:5 to 9:1) resulted in a colorless foam (**13c**: 534 mg, 89%). TLC (silica gel, 9:1 CH_2Cl_2/MeOH) R_f 0.57; UV λ_{max} (MeOH)/nm (ϵ/dm^3 mol^{-1} cm^{-1}) 239 (22 500), 268 (8300), 341 (10 200); ^{1}H NMR (DMSO-d_6, 500 MHz): δ 2.02−2.04 [4H, m, (CH_3)$_2$N(CH_3)C═, H−C(2′)], 2.30−2.35 [1H, m, H−C(2′)], 3.05, 3.10 [6H, 2s, N(CH_3)$_2$], 3.50−3.52 [2H, m, H_2−C(5′)], 3.75−3.78 [1H, m, H−C(4′)], 4.26−4.28 [1H, m, H−C(3′)], 5.06 [1H, br. s, HO−(5′)], 5.24 [1H, d, *J* = 3.9 Hz, HO−C(3′)], 6.26 [1H, 't', *J* = 6.1 Hz, H−C(1′)], 7.22 [1H, s, H−C(6)], 10.96 (1H, br. s, NH); Anal. Calcd for $C_{15}H_{20}BrN_5O_4$ (414.3): C 43.49, H 4.87, N 16.91; found: C 43.52, H 4.76, N 16.61.

7-(2-Deoxy-β-D-*erythro*-pentofuranosyl)-4-[(dimethylaminoethylidene)amino]-2-[(diphenylcarbamoyl)oxy]-7*H*-pyrrolo[2,3-*d*]pyrimidine (14a). General Procedure for the Preparation of 14a−c. To a suspension of compound **13a** (280 mg, 0.84 mmol) in dry pyridine (7.0 mL), diphenylcarbamoyl chloride (254 mg, 1.1 mmol) and *N*,*N*-diisopropylethylamine (0.2 mL, 1.15 mmol) were added and stirred for 1 h at room temperature. Then, the mixture was poured into 5% aqueous $NaHCO_3$ (10 mL) and extracted with CH_2Cl_2 (3 × 10 mL). The CH_2Cl_2 layers were combined, dried over Na_2SO_4, and filtered. After evaporation of the solvent, the residue was applied to FC (silica gel, column 3 × 10 cm). Elution with CH_2Cl_2 followed by CH_2Cl_2/MeOH (98:2 to 95:5) gave **14a** as a colorless foam (401 mg, 91%). TLC (silica gel, 9:1 CH_2Cl_2/MeOH) R_f 0.50; UV λ_{max} (MeOH)/nm (ϵ/dm^3 mol^{-1} cm^{-1}) 233 (35 000), 307 (17 300); ^{1}H NMR (DMSO-d_6, 500 MHz): 2.13 [3H, s, (CH_3)$_2$N(CH_3)C═], 2.20−2.24, 2.44−2.50 [2H, m, H_2−C(2′)], 3.08, 3.12 [6H, 2s, N(CH_3)$_2$], 3.50−3.57 [2H, m, H_2−C(5′)], 3.82−3.85 [1H, m, H−C(4′)], 4.34−4.38 [1H, m, H−C(3′)], 4.95 [1H, 't', *J* = 5.4 Hz, HO−C(5′)], 5.32 [1H, d, *J* = 4.0 Hz, HO−C(3′)], 6.42 [1H, d, *J* = 5.3 Hz, H−C(5)], 6.49 [1H, 't', *J* = 7.2 Hz, H−C(1′)], 7.30−7.45 (10H, m, arom. H), 7.52 [1H, d, *J* = 5.3 Hz, H−C(6)]; Anal. Calcd for $C_{28}H_{30}N_6O_5$ (530.6): C 63.38, H 5.70, N 15.84; found: C 63.56, H 5.80, N 15.73.

5-Chloro-7-(2-deoxy-β-D-*erythro*-pentofuranosyl)-4-[(dimethylaminoethylidene)amino]-2-[(diphenylcarbamoyl)oxy]-7*H*-pyrrolo-[2,3-*d*]pyrimidine (14b). Methods as described for **14a**, with **13b** (320 mg, 0.87 mmol) in dry pyridine (7.0 mL), diphenylcarbamoyl chloride (254 mg, 1.1 mmol), and *N*,*N*-diisopropylethylamine (0.2 mL, 1.15 mmol). The FC (silica gel, column 3 × 10 cm) gave **14b** as a colorless foam (434 mg, 89%). TLC (silica gel, 9:1 CH_2Cl_2/MeOH) R_f 0.51; UV λ_{max} (MeOH)/nm (ϵ/dm^3 mol^{-1} cm^{-1}) 233 (36 800), 312 (15 300); ^{1}H NMR (DMSO-d_6, 500 MHz): 2.16 [3H, s, (CH_3)$_2$N(CH_3)C═], 2.20−2.22, 2.44−2.46 [2H, m, H_2−C(2′)], 3.13 [6H, s, N(CH_3)$_2$], 3.52−3.59 [2H, m, H_2−C(5′)], 3.82−3.85 [1H, m, H−C(4′)], 4.34−4.36 [1H,

m, H−C(3′)], 5.01 [1H, 't', J = 5.4 Hz, HO−C(5′)], 5.34 [1H, d, J = 4.0 Hz, HO− C(3′)], 6.45 [1H, 't', J = 7.2 Hz, H−C(1′)], 7.30−7.45 (10H, m, arom. H), 7.61 [1H, s, H−C(6)]; Anal. Calcd for $C_{28}H_{29}ClN_6O_5$ (565.0): C 59.52, H 5.17, N 14.87; found: C 59.49, H 5.05, N 14.57.

5-Bromo-7-(2-deoxy-*β*-D-*erythro*-pentofuranosyl)-4-[(dimethylaminoethylidene)amino]-2-[(diphenylcarbamoyl)oxy]-7*H*-pyrrolo-[2,3-*d*]pyrimidine (14c). Methods as described for **14a**, with **13c** (476 mg, 1.15 mmol) in dry pyridine (8.0 mL), diphenylcarbamoyl chloride (319 mg, 1.38 mmol), and *N*,*N*-diisopropylethylamine (0.3 mL, 1.72 mmol). The FC (silica gel, column 3 × 10 cm) yielded **14c** as a colorless foam (621 mg, 89%). TLC (silica gel, 9:1 CH_2Cl_2/MeOH) R_f 0.51; UV λ_{max} (MeOH)/nm (ϵ/dm^3 mol^{-1} cm^{-1}) 234 (36 900), 312 (14 400); ^{1}H NMR (DMSO-d_6, 500 MHz): δ 2.15 [3H, s, $(CH_3)_2N(CH_3)C$═], 2.16−2.19, 2.40−2.44 [2H, 2m, H_2−C(2′)], 3.14 [6H, s, $N(CH_3)_2$], 3.52−3.55 [2H, m, H_2−C(5′)], 3.81−3.83 [1H, m, H−C(4′)], 4.33−4.34 [1H, m, H−C(3′)], 5.00 [1H, 't', J = 5.3 Hz, HO−C(5′)], 5.35 [1H, d, J = 3.9 Hz, HO−C(3′)], 6.44 [1H, 't', J = 7.4 Hz, H−C(1′)], 7.30−7.43 (10H, m, arom. H), 7.67 [1H, s, H−C(6)]; Anal. Calcd for $C_{28}H_{29}BrN_6O_5$ (609.5): C 55.18, H 4.80, N 13.79; found: C 55.07, H 5.00, N 13.65.

7-[2-Deoxy-5-*O*-(4,4′-dimethoxytriphenylmethyl)-*β*-D-*erythro*-pentofuranosyl]- 4-[(dimethylaminoethylidene)amino]-2-[(diphenylcarbamoyl)oxy]-7*H*-pyrrolo[2,3-*d*]pyrimidine (15a). A Typical Procedure for the Preparation of 15a−c. Compound **14a** (380 mg, 0.72 mmol) was coevaporated with anhydrous pyridine (three times) and then dissolved in pyridine (2.0 mL). To this solution, 4,4′-dimethoxytriphenylmethyl chloride (313 mg, 0.92 mmol) was added, and the mixture was stirred at room temperature for 5 h. The reaction was quenched by addition of MeOH, and the mixture was evaporated to dryness. It was dissolved in CH_2Cl_2 (3.0 mL) and subjected to FC (column 4 × 9 cm, elution with AcOEt/petroleum ether, 1:2 to 2:3) to give **15a** as a colorless foam (503 mg, 84%). TLC (silica gel, 95:5 CH_2Cl_2/MeOH) R_f 0.36; UV λ_{max} (MeOH)/nm (ϵ/dm^3 mol^{-1} cm^{-1}): 233 (55 800), 282 (12 400), 306 (17 100); ^{1}H NMR (DMSO-d_6, 500 MHz): δ 2.12 [3H, s, $(CH_3)_2N(CH_3)C$═], 2.21−2.27, 2.48−2.52 [2H, 2m, H_2−C(2′)], 3.08−3.12 [8H, m, H_2−C(5′), $N(CH_3)_2$], 3.71 (6H, s, 2 CH_3O), 3.90−3.92 [1 H, m, H−C(4′)], 4.333−4.36 [1H, m, H−C(3′)], 5.36 [d, J = 4.5 Hz, HO−C(3′)], 6.38 [1H, d, J = 3.7 Hz, H−C(5)], 6.49 [1H, 't', J = 7.2 Hz, H−C(1′)], 6.81−7.37 (23H, m, arom. H), 7.42 [1H, d, J = 3.7 Hz, H−C(6)]. Anal. Calcd for $C_{49}H_{48}N_6O_7$ (832.9): C 70.66, H 5.81, N 10.09; found: C 70.58, H 5.85, N 9.99.

5-Chloro-7-[2-deoxy-5-*O*-(4,4′-dimethoxytriphenylmethyl)-*β*-D-*erythro*-pentofuranosyl]- 4-[(dimethylaminoethylidene)amino]-2-[(diphenylcarbamoyl)oxy]-7*H*-pyrrolo[2,3-*d*]pyrimidine (15b). Methods as described for **15a**, with **14b** (400 mg, 0.71 mmol) in anhydrous pyridine (2.0 mL) and 4,4′-dimethoxytriphenylmethyl chloride (313 mg, 0.92 mmol). FC (column 4 × 9 cm, elution with AcOEt/petroleum ether, 1:2 to 2:3) resulted in **15b** as a colorless foam (491 mg, 80%). TLC (silica gel, 95:5 CH_2Cl_2/MeOH) R_f 0.36; UV λ_{max} (MeOH)/nm (ϵ/dm^3 mol^{-1} cm^{-1}): 234 (55 700), 275 (12 100), 311 (15 000); ^{1}H NMR (DMSO-d_6, 500 MHz): δ 2.15 [3H, s, $(CH_3)_2N(CH_3)C$═], 2.25−2.29, 2.50−2.51 [2H, 2m, H−C(2′)], 3.12−3.13 [8H, m, H−C(5′), $N(CH_3)_2$], 3.71 (6H, s, 2 CH_3O), 3.90−3.91 [1H, m, H−C(4′)], 4.36−4.38 [1H, m, H−C(3′)], 5.41 [d, J = 4.0 Hz, HO−C(3′)], 6.48 ['t', J = 5.9 Hz, H−C(1′)], 6.81−7.42 (23H, m, arom. H), 7.46 [s, H−C(6)]. Anal. Calcd for $C_{49}H_{47}ClN_6O_7$ (867.4): C 67.85, H 5.46, N 9.69; found: C 68.15, H 5.64, N 9.80.

5-Bromo-7-[2-deoxy-5-*O*-(4,4′-dimethoxytriphenylmethyl)-*β*-D-*erythro*-pentofuranosyl]-4-[(dimethylaminoethylidene)amino]-2-[(diphenylcarbamoyl)oxy]-7*H*-pyrrolo[2,3-*d*]pyrimidine (15c). Compound **14c** (400 mg, 0.66 mmol) was used, and **15c** was obtained as a colorless foam (493 mg, 82%). TLC (silica gel, 95:5 CH_2Cl_2/MeOH) R_f 0.36; UV λ_{max} (MeOH)/nm (ϵ/dm^3 mol^{-1} cm^{-1}): 234 (55 600), 275 (11 800), 312 (14 200); ^{1}H NMR (DMSO-d_6, 500 MHz): δ 2.13 [3H, s, $(CH_3)_2N(CH_3)C$═], 2.14−2.16, 2.48−2.50 [2H, m, H−C(2′)], 3.12−3.14 [8H, m, H_2−C(5′), $N(CH_3)_2$], 3.69 (6H, m, 2 CH_3O), 3.91−4.00 [1H, m, H−C(4′)], 4.35−4.36 [1H, m, H−C(3′)], 5.38−5.39 [1H, m, HO−C(3′)], 6.46 ['t', J = 5.9 Hz, H−C(1′)], 6.81−7.42 [23H, m, arom. H], 7.49 [s, H−C(6)]; Anal. Calcd for $C_{49}H_{47}BrN_6O_7$ (911.8): C 64.54, H 5.20, N 9.22; found: C 64.57, H 5.25, N 9.15.

7-[2-Deoxy-5-*O*-(4,4′-dimethoxytriphenylmethyl)-*β*-D-*erythro*-pentofuranosyl]-4-[(dimethylaminoethylidene)amino]-2-[(diphenylcarbamoyl)oxy]-7*H*-pyrrolo[2,3-*d*]pyrimidine 3′-(2-cyanoethyl)-*N*,*N*-diisopropylphosphoramidite (5). A Typical Procedure for the Preparation of 5−7. Compound **15a** (450 mg, 0.54 mmol) dissolved in anhydrous CH_2Cl_2 (3.0 mL) under Ar atmosphere was reacted with 2-cyanoethyl-*N*,*N*-diisopropylchlorophosphoramidite (150 μL, 0.67 mmol) in the presence of (^{i}Pr)$_2$NEt (130 μL, 0.25 mmol) at room temperature. After 30 min, the reaction mixture was diluted with CH_2Cl_2, and the solution was washed with a 5% aqueous $NaHCO_3$ solution, followed by brine. The organic solution was dried over Na_2SO_4 and concentrated, and the residue was submitted to FC (column 3 × 9 cm, CH_2Cl_2/acetone, 98:2), yielding a colorless foam (508 mg, 91%). TLC (silica gel, 97:3 CH_2Cl_2/acetone) R_f 0.22, 0.25; ^{31}P NMR ($CDCl_3$, 500 MHz): δ 149.9, 149.7.

5-Chloro-7-[2-deoxy-5-*O*-(4,4′-dimethoxytriphenylmethyl)-*β*-D-*erythro*-pentofuranosyl]- 4-[(dimethylaminoethylidene)amino]-2-[(diphenylcarbamoyl)oxy]-7*H*-pyrrolo[2,3-*d*]pyrimidine 3′-(2-cyanoethyl)-*N*,*N*-diisopropylphosphoramidite (6). Methods as described for **5**, with compound **15b** (360 mg, 0.42 mmol) in anhydrous CH_2Cl_2 (3.0 mL), 2-cyanoethyl-*N*,*N*-diisopropylchlorophosphoramidite (130 μL, 0.58 mmol), and (^{i}Pr)$_2$NEt (130 μL, 0.75 mmol). The FC (column 3 × 9 cm, CH_2Cl_2/acetone, 98:2) yielded a colorless foam (412 mg, 93%). TLC (silica gel, 97:3 CH_2Cl_2/acetone) R_f 0.23, 0.27; ^{31}P NMR ($CDCl_3$, 500 MHz): δ 149.9, 149.8.

5-Bromo-7-[2-deoxy-5-*O*-(4,4′-dimethoxytriphenylmethyl)-*β*-D-*erythro*-pentofuranosyl]-4-[(dimethylaminoethylidene)amino]-2-[(diphenylcarbamoyl)oxy]-7*H*-pyrrolo[2,3-*d*]pyrimidine 3′-(2-cyanoethyl)-*N*,*N*-diisopropylphosphoramidite (7). Method as described for **5**, with compound **15c** (430 mg, 0.47 mmol) in anhydrous CH_2Cl_2 (6.0 mL), 2-cyanoethyl-*N*,*N*-diisopropylchlorophosphoramidite (150 μL, 0.67 mmol), and (^{i}Pr)$_2$NEt (148 μL, 0.85 mmol) under Ar. Compound **7** was obtained as a colorless foam (470 mg, 90%). TLC (silica gel, 97:3 CH_2Cl_2/acetone) R_f 0.24, 0.28; ^{31}P NMR ($CDCl_3$, 500 MHz): 149.9, 149.8.

Oligonucleotides Synthesis. The oligonucleotides **16**−**52** were prepared in a 1 μmol scale (trityl on mode) on an ABI 392-08 synthesizer employing phosphoramidite chemistry.[24] The phosphoramidites **5**−**7**, 5′-*O*-DMT-*N*^{2}-[(dimethylamino)methylidene]-2′-deoxy-5-methylisocytidine 3′-*O*-(2-cyanoethyl)phosphormidite,[4d] as well as standard phosphoramidites were employed in solid-phase synthesis. The average coupling yield of the modified phosphoramidites **5**−**7** was always higher than 95%. After cleavage from the solid support, the oligonucleotides were deprotected in 25% aqueous NH_3 for 20−24 h at 60 °C. The DMT-containing oligonucleotides were purified by reversed-phase HPLC (RP-18) with the following solvent gradient system [A: 0.1 M (Et_3NH)OAc (pH 7.0)/MeCN 95:5; B: MeCN; gradient *I*: 0−3 min 10−15% B in A, 3−15 min 15−50% B in A, 15−20 min 50−10% B in A, flow rate 1.0 mL/min]. Then, the mixture was evaporated to dryness, and the residue was treated with 2.5% $Cl_2CHCOOH/CH_2Cl_2$ for 4 min at room temperature to remove the 4,4′-dimethoxytrityl residues. The detritylated oligomers were purified by reversed-phase HPLC with the gradient *II*: 0−25 min 0−20% B in A, 25−30 min 20% B in A, 30−35 min 20−0% B in A, flow rate 1.0 mL/min. The oligomers were desalted on a short column (RP-18, silica gel) using H_2O for elution of the salt, while the oligomers were eluted with MeOH/H_2O 3:2. The oligonucleotides were lyophilized on a Speed Vac evaporator to yield colorless solids that were stored frozen at −18 °C. Although the monomers of 7-deazpurines are more easily oxidized than purines, no degradation was found when oligonucleotides were

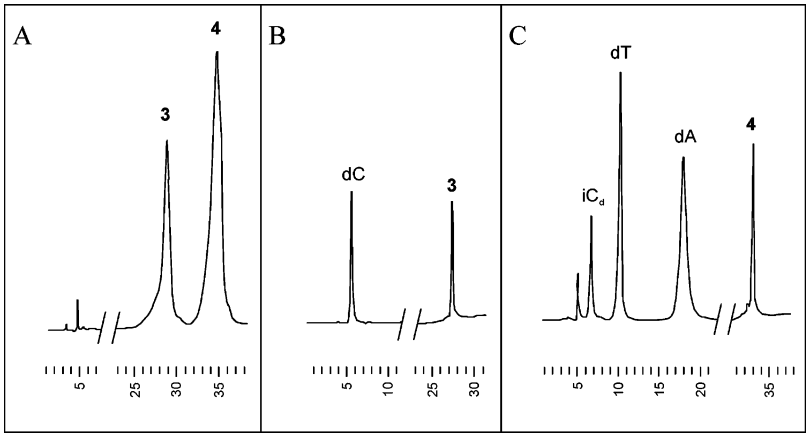

Figure 10. HPLC profiles of the nucleosides **3** and **4** (A) and HPLC profiles of the enzymatic analysis of the oligonucleotide **18** (B) containing nucleoside **3** and oligonucleotide **36** (C) containing nucleoside **4**, obtained by digestion with snake venom phosphodiesterase followed by alkaline phosphatase in 0.1 M Tris·HCl buffer (pH 8.3) at 37 °C. The nucleoside mixtures were analyzed by reversed-phase HPLC at 260 nm on a RP-18 column (200 × 10 cm). Gradient: 0−20 min 100% A, 20−40 min 0−65% B in A, 40−60 min 65−0% B in A, flow rate 0.7 mL/min [A: 0.1 M (Et_3NH)OAc (pH 7.0)/MeCN 95:5; B: MeCN] ($^{Me}iC_d$ = 5-methyl-2′-deoxyisocytidine).

Table 8. Molecular Masses Determined from MALDI-TOF Mass Spectra and Extinction Coefficients of Oligonucleotides

	MH$^+$ (calcd)	MH$^+$ (found)	$\epsilon_{260}{}^b$ (M^{-1} cm^{-1})	$\epsilon_{260}{}^c$ (M^{-1} cm^{-1})
5′-d(**1**T)$_6$-3′ (**20**)	3739.2	3739.8	78 600	62 900
5′-d(**2**T)$_6$-3′ (**22**)	3733.2	3734.5	97 200	87 500
5′-d(**3**C**3**C**3**C)-3′ (**18**)	1894.6	1894.9	42 000	37 800
5′-d(**3**T)$_6$-3′ (**23**)	3940.2	3940.6	91 200	86 600
5′-d(AGTATT**3**ACCTA)-3′ (**40**)	3678.9	3680.4	130 200	104 200
5′-d(TAG**3**TCAATACT)-3′ (**51**)	3678.9	3680.4	130 200	104 200
5′-d(ATiCiCA**3**TTAT**3**A)-3′ (**35**)^a	3740.5	3741.2	122 200	110 000
5′-d(TiCATAAiCT**33**AT)-3′ (**30**)^a	3740.5	3740.2	122 200	110 000
5′-d(**4**C**4**C**4**C)-3′ (**19**)	2027.9	2029.3	40 200	36 200
5′-d(**4**T)$_6$-3′ (**24**)	4206.9	4207.2	87 600	83 200
5′-d(AGTATT**4**ACCTA)-3′ (**41**)	3723.4	3723.7	129 500	103 600
5′-d(TAG**4**TCAATACT)-3′ (**52**)	3723.4	3724.2	129 500	103 600
5′-d(ATiCiCA**4**TTAT**4**A)-3′ (**36**)^a	3827.5	3827.6	121 000	108 900
5′-d(TiCATAAiCT**44**AT)-3′ (**31**)^a	3827.5	3828.2	121 000	108 900
5′-d(CA)$_6$-3′ (**21**)	3553.1	3552.9	138 000	110 400
5′-d(GT)$_6$-3′ (**25**)	3739.2	3740.1	123 000	98 400
5′-d(AGTATTGACCTA)-3′ (**28**)	3645.4	3645.2	135 400	108 300
5′-d(TAGGTCAATACT)-3′ (**33**)	3645.4	3645.2	135 400	108 300

^{a} d(iC) = $^{Me}iC_d$ = 5-methyl-2′-deoxyisocytidine. ^{b} Calculated extinction coefficients. ^{c} The extinction coefficients corrected by the hypochromicity.

stored for longer periods or when measurements were performed as described in the manuscript.

Oligonucleotides Characterization. The nucleoside composition of oligomers was determined by enzymatic hydrolysis with snake venom phosphodiesterase (EC 3.1.15.1, *C. adamanteus*) followed by alkaline phosphatase (EC 3.1.3.1, *E. coli* from Roche Diagnostics GmbH, Germany). The mixture was analyzed on reversed-phase HPLC (RP-18) (Figure 10). The absorbances were quantified at 260 nm by measuring the peak areas under consideration of the molar extinction coefficients of each monomer (ϵ_{260}: c^7iG_d 7400, $Cl^7c^7iG_d$ 6400, Br^7c^7-iG_d 5800, iG_d 4300, dA 15 400, dT 8800, dG 11 700, dC 7600, m^5iC_d 6300). Figure 10A indicates brominated nucleoside **4** is more hydrophobic than compound **3**. Figure 10B,C shows the HPLC profiles of the enzymatic hydrolysates of the oligonucleotides **18** and **36**. Quantification of the material was made on the basis of the peak areas, which were divided by the extinction coefficients of the nucleoside constituents (Figure 10). The peak areas of oligonucleotide **18** are 840 633 for dC and 766 055 for compound **3**, then dC/**3** = 1.1:1. In the case of oligonucleotide **36**: m^5iC_d (1 479 552), dT (4 138 803), dA (6 789 902), nucleoside **4** (1 460 000), accordingly m^5iC_d/dT/dA/**4** equals 1:2:1.9:1.1.These data fit with the calculated data, which shows that the oligonucleotides were completely hydrolyzed.

The molecular masses of all synthesized oligonucleotides were determined by MALDI-TOF mass spectra measured on a Biflex-III spectrometer in the reflector mode (Bruker Saxonia, Leipzig, Germany). They were in agreement with the calculated values (Table 8).

Thermodynamic Measurements. UV thermal denaturation curves were measured on a Cary 1/3 UV/vis spectrophotometer (Varian, Australia) equipped with a Cary thermoelectrical controller. All measurements were performed in 1.0 M NaCl, 0.1 M $MgCl_2$, and 60 mM Na-cacodylate buffer, at pH 7.0 ± 0.2, with 5 μM + 5 μM single-strand concentration. The concentrations of the oligonucleotides were determined by measuring the absorbances at 260 nm. The extinction coefficients at 260 nm of the oligonucleotides were calculated from the sum of the extinction coefficients of the monomeric 2′-deoxyribonucleosides corrected by the hypochromicity (Table 8). The hypochromicity ($h = [(\epsilon_{monomer} - \epsilon_{polymer}) \cdot (\epsilon_{monomer})^{-1}] \cdot 100\%$) was determined from the absorbance before and after enzymatic digestion with SVPD. The hypochromicity was 20% for unmodified oligonucleotides or for those with one modification (**20**, **21**, **25**, **28**, **33**, **40**, **41**, **51**, and **52**), 10% for highly modified oligonucleotides (**18**, **19**, **22**, **30**, **31**, **35**, and **36**), and around 5% for compounds **23** and **24**. Absorbance versus temperature spectra were collected at 260 nm over a range of 10−95 °C with 0.1 °C increments and a heating rate of 1.0 °C/min. Samples were annealed by heating rapidly to 95 °C for 10−15 min, followed by cooling slowly to 10 °C. The thermodynamic data were calculated using the program Meltwin 3.0.[29]

(29) McDowell, J. A.; Turner, D. H. *Biochemistry* **1996**, *35*, 14077−14089.

Acknowledgment. We thank Dr. Helmut Rosemeyer and Dr. Xiaomei Zhang for the measurement of the NMR spectra, Dr. Peter Leonard for the supply of nucleobase precursors, Dr. Yang He for the synthesis of the oligonucleotides, and Khalil I. Shaikh for the MALDI-TOF mass spectra. We also appreciate the assistance of Mrs. Monika Dubiel and Mrs. Elisabeth Michalek during the preparation of the manuscript. Financial support by Roche Diagnostics GmbH, Germany, is gratefully acknowledged.

Supporting Information Available: The half-life measurement of compound **12**. The synthesis of the fixed-keto compound **4k** and the fixed-enol isomer **4e**. pK_a measurements of compounds **2**−**4**. Determination of the tautomeric equilibrium data of compounds **2**−**4**. This material is available free of charge via the Internet at http://pubs.acs.org.

JA0425785